4
Anode Catalysts for Low-Temperature Direct Alcohol Fuel Cells

Wenzhen Li

4.1
Introduction

Low-temperature polymer electrolyte fuel cells are promising electrochemical energy devices that can directly transform the chemical energy stored in a fuel (e.g., H_2 and alcohols) into electrical energy with low emission and high efficiency [1–8]. This electrochemical process does not obey Carnot cycle limitation, so higher energy efficiencies can be achieved through fuel cells: 40–50% in electrical energy and 80–85% in total energy (electricity + heat production) [6]. Hydrogen is considered the most convenient fuel for vehicle applications, because the kinetics of hydrogen oxidation is very fast and the product is only water. However, hydrogen itself is merely an energy carrier, not a natural resource. The production, transportation, and storage of hydrogen have encountered huge technical challenges [9]. Compared with hydrogen, small liquid alcohol fuels have obvious advantages, including high energy density and thermodynamic energy conversion efficiency, comparable electromotive force (thermodynamic potential), and complete elimination of hydrogen production and storage accessories [1,6,7]. In addition, many alcohols can be massively obtained from renewable biomass feedstocks [10–12]. For example, methanol can be produced from fermentation of agricultural products from biomass; ethanol is one of the major fuels obtained from agriculture fermentation (first-generation bioethanol); ethylene glycol (EG) can be obtained in large quantity by heterogeneous hydrogenation of cellulose; and glycerol is a main by-product of biodiesel production. They are potentially cheap and abundant, and can be widely distributed by using the present infrastructures for liquid fuels. Therefore, low-temperature direct alcohol fuel cells (DAFCs) have emerged as clean and sustainable mobile power sources for portable electronics, and potentially for transportation systems.

Table 4.1 shows the thermodynamic properties of selected alcohol fuels at standard conditions. Although their electromotive forces are slightly lower than

Materials for Low-Temperature Fuel Cells, First Edition. Edited by Bradley Ladewig, San P. Jiang, and Yushan Yan.

Table 4.1 The transferred electrons (N_e), electromotive force (E°), volume energy density (W_e), and thermodynamic energy conversion efficiency (ε_{rev}) of electrooxidation of selected alcohols at standard conditions.

Fuel	N_e	E° (V)	W_e (kW h l^{-1})	ε_{rev} (%)
Hydrogen	2	1.23	2.6 (liquid H_2)	83
Methanol	6	1.18	4.8	97
Ethanol	12	1.15	6.3	97
Ethylene glycol	10	1.22	5.9	99
Glycerol	14	1.22	6.3	99

hydrogen, the thermodynamic energy conversion efficiencies of methanol, ethanol, ethylene glycol, and glycerol are in the range of 97–99%, which is higher than that of hydrogen (83%). The mass and volume energy densities of the alcohols are also higher than that of hydrogen.

Despite their attractive thermodynamic advantages and practical system benefits, current direct alcohol fuel cells have the significant disadvantage of having lower output power density and efficiency than hydrogen–proton exchange membrane fuel cells (PEMFCs). Besides the urgent need for the development of advanced polymer membranes that can reduce both enhanced ion conductivity and alcohol crossover, the sluggish alcohol reaction kinetics must be significantly improved for widespread applications of DAFCs. For instance, the overpotential of methanol oxidation is >0.3 V at 0.5 A cm^{-2} on the state-of-the-art PtRu/C catalyst, which is much higher than hydrogen oxidation reaction (only 0.02 V) [4]. The ethanol oxidation has a similar slow kinetics. More serious, since the C−C bond of ethanol is difficult to break at low temperatures (e.g., <90 °C), the major electrooxidation products are acetaldehyde and acetic acid, and CO_2 is only <10% on the current PtSn catalysts [6,13]. The incomplete ethanol oxidation leads to low ethanol utilization and energy conversion efficiency.

Efficient direct transformation of chemical energy stored in small organic molecules into electricity has been a long-term goal for scientists. Significant research efforts have been made in recent decades to acquire a deep understanding of the mechanisms of electrocatalytic oxidation of alcohols, and to further develop more efficient anode catalysts for DAFCs. This chapter focuses on anode catalytic materials for low-temperature DAFCs. First, the acquired knowledge of electrooxidation of alcohols (methanol, ethanol, ethylene glycol, and glycerol) in both acid and alkaline media, and state-of-the-art anode catalysts are presented. Second, the recently developed catalyst preparation methods and novel carbon support materials are reviewed. Finally, the future research challenges and opportunities in this field are discussed.

4.2
Anode Catalysts for Direct Methanol Fuel Cells: Improved Performance of Binary and Ternary Catalysts

4.2.1
Principles of Direct Methanol Fuel Cells

A typical proton exchange membrane (PEM)-based direct methanol fuel cell comprises anode, PEM, and cathode. At the anode, methanol is oxidized to produce CO_2; at the cathode, oxygen reacts with protons and electrons to produce water:

$$CH_3OH + H_2O \rightarrow CO_2 + 6H^+ + 6e^- \quad +0.05\,\text{V versus SHE} \quad \text{(anode)} \qquad (4.1)$$

$$3/2O_2 + 6H^+ + 6e^- \rightarrow 3H_2O \quad +1.23\,\text{V versus SHE} \quad \text{(cathode)} \qquad (4.2)$$

The total reaction is

$$CH_3OH + 3/2O_2 \rightarrow CO_2 + 2H_2O \quad +1.18\,\text{V} \qquad (4.3)$$

4.2.2
Reaction Mechanisms and Catalysts for Methanol Electrooxidation

In the past decades, a significant number of fundamental investigations have been carried out in the field of low-temperature electrooxidation of small organic molecules [14–38]. Electrochemical studies have been carried out in combination with spectroscopy [21,27,28], mass spectroscopy [25,31], physiochemical tools [20,30], as well as theoretical calculations (e.g., DFT) [38] in order to examine the adsorbed species and reactive intermediates on the electrode surface during the alcohol oxidation, and thus to elucidate the alcohol reaction pathways.

From a general point of view, at ambient pressure and temperature, all electrooxidations of short-chain aliphatic alcohols (in acid) require the presence of the expensive precious metal Pt. However, as is well known, Pt is readily poisoned by CO-like intermediate species formed during methanol oxidation at low temperatures. It has been found that Pt-based binary or ternary catalysts, Pt-M_1, Pt-M_1-M_2 (M = Ru, Sn, etc.) can improve the reaction kinetics of methanol electrooxidation based on the bifunctional effect (promoted mechanism by the second metal) [17,19,22,24,26] and/or on the tuned electronic properties of Pt (the intrinsic mechanism) [28,29,36]. The bifunctional effect is illustrated in the following equations:

$$Pt + CH_3OH \rightarrow Pt - (CH_3OH)_{ads} \qquad (4.4)$$

$$Pt - (CH_3OH)_{ads} \rightarrow Pt - (CO)_{ads} + 4H^+ + 4e^- \qquad (4.5)$$

$$M + H_2O \rightarrow M - (H_2O)_{ads} \qquad (4.6)$$

$$M-(H_2O)_{ads} \rightarrow M-(OH)_{ads} + H^+ + e^- \tag{4.7}$$

$$Pt-(CO)_{ads} + M-(OH)_{ads} \rightarrow Pt + M + CO_2 + H^+ + e^- \tag{4.8}$$

After methanol adsorption on Pt catalysts, dehydrogenation (C—H bond cleavage or C—H activation) of methanol proceeds to produce $CO_{(ads)}$. Equations 4.6 and 4.7 relate to water activation on M. Pt and M cooperate to oxidize $CO_{(ads)}$ to yield CO_2 (Equation 4.8). The rate-determining step has long been thought to be within these steps (4.6)–(4.8). It is worth mentioning that using DFT and single-crystal model catalyst, Wieckowski and coworkers have calculated the energetic for CH_3OH dehydrogenation steps and elucidated that methanol dehydrogenation (Equation 4.5) proceeds via the following reaction path [38]:

$$\begin{aligned} CH_3OH_{ads} &\rightarrow CH_2OH_{ads} + H_{ads} \rightarrow CHOH_{ads} + 2H_{ads} \\ &\rightarrow COH_{ads} + 3H_{ads} \rightarrow CO_{ads} + 4H_{ads} \end{aligned} \tag{4.9}$$

The intrinsic mechanism states that M could modify the electronic properties of Pt, and as a consequence, change the adsorption of oxygen-containing species and even the dissociative adsorption of methanol. The CO adsorption on Pt is stabilized by two simultaneous effects: electron transfer (donation) from the CO-filled 5σ molecular orbital to the empty dσ band of Pt, and back-donation of electrons from metal dπ orbital to empty $2\pi^*$ antibonding orbital of CO. The generation of an σ-type bond strengthens the p-type bond and vice versa. In the Pt–M alloys, a modification of the empty electron state density of Pt occurs, with a shift of the Fermi energy level with respect to the energy of CO molecular orbital. This generates the synergistic effect to weaken the Pt—CO bond, and thus facilitates the methanol oxidation kinetics.

Among all the Pt-based alloys, PtRu was found to be the best candidate catalysts for methanol eletrooxidation [17,18,39–41]. The composition and structure of PtRu strongly affect the catalytic activity. It has been reported that 40–60 at.% Ru gives the optimum catalytic activity to methanol oxidation. In the early study, synthesis of PtRu alloy was emphasized, because Ru sites are required to locate close to Pt sites to promote oxidation of CO (Equation 4.10), according to the bifunctional mechanism. In addition, a closer Pt–Ru interaction will promote electronic effects of Pt, which could lead to facile removal of CO_{ads}. With the advancement of research, it was found that the formation of a PtRu alloy was not an essential requirement for a high methanol oxidation activity. Rolison *et al.* found that if Ru existed as hydrous oxide, the methanol oxidation activity would be greatly improved [42–44]. Ren *et al.* also showed that the more RuO_xH_y content, the better the DMFC performance [45]. The benefits of RuO_xH_y were attributed to the conductivity of its electrons and protons and the innate possession of surface OH groups. Although the preferable Ru form is still under debate, it is encouraging to find that PtRu-based ternary and quarterly catalysts can further improve methanol oxidation activity. Experimental and combinational high-throughput methods

have been employed and it has been found that the "promotional" elements include W, Mo, Ir, Os, Ni, Co, V, Rh, and so on. Reddington *et al.* demonstrated that $Pt_{44}Ru_{41}Os_{10}Ir_5$ is the best composition in both half-cell and single DMFC tests among more than 600 Pt–Ru–Os–Ir quaternary catalysts [33]. Kim *et al.* found that PtRuSn is a better catalyst than PtRu, and ascribed the enhancement of MOR activity to the synergistic effects of Ru as a water activator and Sn as an electronic modifier of Pt [46]. It was noted that the third and fourth element amount should be kept lower than a certain amount, otherwise its presence will have a negative effect on the catalyst performance. In general, Pt–Sn catalysts present a higher CO oxidation activity, but lower methanol oxidation activity, probably due to a decreased methanol adsorption and dehydrogenation on Pt–Sn. Binary Pt–W, Pt–Ni, and Pt–Co catalysts have also demonstrated a certain degree of MOR improvement than pure Pt, but the activity improvement is less than PtRu [47–49].

The development of direct methanol fuel cell technology in the last decades has achieved very interesting results. The peak power density of a PEM-based DMFC can reach 500 mW cm^{-2} and 300 mW cm^{-2} under oxygen and air feed operation, respectively. At a fuel cell voltage of 0.5 V, 200 mW cm^{-2} has been reported at a temperature close to or above 100 °C under pressured conditions, with a Pt loading of 1–2 mg cm^{-2}. However, at ambient temperature and passive air-breathing mode operation, the power density range remains between 10 and 40 mW cm^{-2} [4]. The high energy density of DMFCs makes them a competitive replacement of current Li ion batteries for a global portable electronics market of 6 billion dollars. As a comparison, the alkaline membrane-based DMFC has a much lower performance than peak power density, that is, ~80 mW cm^{-2} for Pd/multiwalled nanotubes (MWNTs) anode DMFC [50]. Therefore, the alkaline membranes have more advantages for direct C_{2+} alcohol fuel cells, as discussed in the following sections.

4.3 Anode Catalysts for Direct Ethanol Fuel Cells: Break C—C Bond to Achieve Complete 12-Electron-Transfer Oxidation

Ethanol is a biorenewable molecule. It is manufactured through photosynthesis causing an agricultural feedstock, such as sugarcane, corn, grain, wheat, cotton, and many types of cellulose wastes and harvests. Using ethanol as fuel has a big advantage of reducing CO_2 footprints in the atmosphere, because the absorption of CO_2 by living plant matter will be used as the feedstock to produce it [51]. The current utilization of ethanol fuel is as blends of gasoline with denatured ethanol, that is, E85 is 85% ethanol-mixed gasoline, which has recently appeared at fueling stations in the United States, mainly in the Midwest. However, all internal combustion engines are limited by the Carnot cycle. In principle, generation of electricity through direct ethanol fuel cells is a more efficient way to utilizing ethanol [6].

4.3.1 Principles of PEM-Direct Ethanol Fuel Cells

In an acid electrolyte, the anode, cathode, and overall reactions are as follows:

$$C_2H_5OH + 3H_2O \rightarrow 2CO_2 + 12H^+ + 12e^- \quad +0.085\,\text{V versus SHE} \quad \text{(anode)} \tag{4.10}$$

$$3O_2 + 12H^+ + 12e^- \rightarrow 6H_2O \quad +1.23\,\text{V versus SHE} \quad \text{(cathode)} \tag{4.11}$$

$$C_2H_5OH + 3O_2 \rightarrow 2CO_2 + 3H_2O \quad +1.15\,\text{V} \quad \text{(overall)} \tag{4.12}$$

The thermodynamic reversible energy efficiency at standard conditions is 97%, which is defined as the ratio of the electrical energy produced, and the heat of the combustion at constant pressure. However, under the working conditions, with a current j, the cell voltage is lower than the equilibrium potential; therefore, the practical energy efficiency is lower. For example, for a direct ethanol fuel cell working at 0.55 V and 100 mA cm^{-2} with 80% selectivity to CO_2 and 20% selectivity to acetic acid, the efficiency is

$$\varepsilon_{\text{cell}} = \varepsilon_F \times \varepsilon_E \times \varepsilon_{\text{rev}} = (0.2 \times 4/12 + 0.8 \times 1) \times (0.55/1.15) \times 0.97 = 40\%$$

The potential efficiency $\varepsilon_E = 48\%$ (0.55/1.15). The Faradic efficiency ε_F is associated with the product distribution (catalyst selectivity). For CO_2 product, the Faradic efficiency is 100% (12/12), while for acetic acid product, only four electrons are transferred, and the Faradic efficiency is 33% (4/12). Although higher current densities are not necessarily associated with complete oxidation of ethanol, improving the anode catalyst selectivity to CO_2 will increase the overall DEFC efficiency and fuel utilization.

4.3.2 Reaction Mechanisms and Catalysts for Ethanol Electrooxidation

The complete electrooxidation of ethanol is a complex 12-electron-transfer reaction and various reaction intermediates can be formed during the ethanol oxidation process. The electrochemical oxidation of ethanol in acid electrolyte requires Pt, which is primarily involved in two key steps – cleavage of C−H and C−C bonds – occurring during the oxidation process.

Based on half-cell and single fuel cell tests, *in situ* FTIR spectroscopy, and chromatograph studies, a proposed overall scheme for ethanol oxidation on Pt-based catalysts is summarized in Figure 4.1 [52]. The first step is the dissociative adsorption of ethanol through either O-adsorption or C-adsorption (step 1) [53,54], leading to the formation of adsorbed acetaldehyde (step 2). Acetaldehyde has been examined at potential <0.6 V versus RHE. It could be readsorbed according to step 3 and react with adsorbed OH to generate acetic acid through a bifunctional mechanism as shown in step 4. This step does not break the C−C bond and often occurs at >0.6 V RHE. The adsorbed CH_3CHOH could also undergo further dehydrogenation (step 5) and react with adsorbed OH to

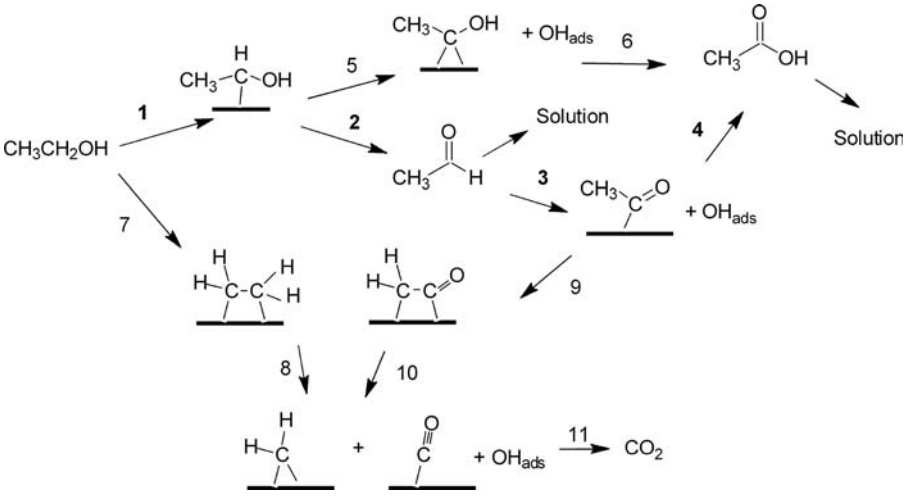

Figure 4.1 Proposed mechanisms for ethanol oxidation reaction [52].

produce acetic acid directly (step 6) [6]. There is still some controversy on whether acetic acid is formed through acetaldehyde or through CH_3COH (steps 5 and 6).

Pt is able to break the C−C bond, leading to adsorbed CO species at relatively low anode potentials: from 0.3 V RHE, the adsorbed peak has clearly been shown in SNIFTIRS spectrum [55]. One can consider two distinct sequences: steps 7 and 8 or steps 9 and 10. The first sequence assumes that ethanol must be adsorbed by the C−H bond cleavage in both carbon atoms and the second sequence assumes that the rupture of the C−H bond of the intermediate formed after the acetaldehyde adsorption. The CO_{ads} species thus react with adsorbed OH to produce CO_2 through step 11. Trace amount of CH_4 at the potential of <0.4 V has been detected, thus the following reaction may occur [53,54]:

$$\mathrm{Pt-(COCH_3)_{ads} + Pt \rightarrow Pt-(CO)_{ads} + Pt-(CH_3)_{ads}}, \quad \text{at } E > 0.3\,\mathrm{V\ SHE} \tag{4.13}$$

$$\mathrm{Pt-(CH_3)_{ads} + Pt-(H)_{ads} \rightarrow 2Pt + CH_4}, \quad \text{at } E < 0.4\,\mathrm{V\ SHE} \tag{4.14}$$

It is interesting to note that only acetic acid, acetaldehyde, and CO_2 have been detected by HPLC from the outlet of the anode compartment of a DEFC with Pt/C catalyst [56], while depending on electrode potentials, acetaldehyde, acetic acid, CO_2, and trace amounts of CH_4 can be found in electrolysis half-cell. It is also found that acetaldehyde can be exclusively produced at a potential <0.35 V versus RHE on a Pt catalyst in a long-time electrolysis experiment; no acetic acid was detected in the potential range [6]. This implies that the alcohol product distribution depends on electric energy input.

In an acid electrolyte, Pt-based catalysts have shown better EOR activity than other platinum group metal (PGM)-based ones. However, Pt itself is readily poisoned by various C_1, C_2 intermediate species. Binary and ternary Pt-based

catalysts, including Ru, Sn, Pb, Pd, and so on, have been thoroughly investigated to improve the kinetics of ethanol oxidation. Sn appeared to be the most promising one [2,7,57–59]. Xin Lab has examined Pt–M (M = Ru, Sn, Pd, and W) catalysts in single PEM-DEFC and found the activity order to be PtSn > PtRu > PtPd > Pt. W and Mo were also alloyed with Pt_1Ru_1 catalysts and still show inferior EOR activity compared with PtSn [60–65]. Lamy and coworkers studied PtSn/C(90 : 10, 50 : 50), PtRu/C(90 : 10, 80 : 10), and $Pt_{86}Sn_{10}Ru_4$/C and demonstrated that PtSn has a much higher EOR activity than Pt [52,56,66,67]. The product distributions of EOR on PtSn catalysts, however, have been changed compared with Pt:An increase in the acetic acid yield and a decrease in acetaldehyde and CO_2 yield. The presence of Sn seems to allow the activation of water molecules and the oxidation of acetaldehyde species into acetic acid at low potentials through bifunctional mechanism. At the same time, Sn dilutes the adjacent Pt atom concentration, thus decreasing the possibility of dissociative adsorption of ethanol with two carbons, which can directly lead to CO_2 production. The function of Sn may also include some electronic effects (ligand effect) on the CO oxidation reaction [68]. Wang *et al.* studied Pt/C, PtRu/C, and Pt_3Sn/C using *in situ* FTIR spectroscopy and online DEMS studies, and also found that the additions of Ru and Sn do not promote C−C bond cleavage, and that the total CO_2 production was <2% contributed to current [13]. Therefore, the previous work shows that the higher ethanol oxidation current density on the PtSn/C catalysts results from higher yields of C_2 products, not from improved complete ethanol oxidation to CO_2.

The recent research efforts are toward discovering new catalyst compositions and structures that can simultaneously break C−C bond to achieve complete EOR and to increase (or at least maintain) the EOR activity. The addition of Rh to Pt seems to promote the C−C bond breakage, however, the overall EOR activity is lower than PtSn [69,70]. Adzic and coworkers group recently demonstrated that a ternary Pt/Rh/SnO_2 nanostructured catalyst can better break C−C bond and promote EOR kinetics [71]. The EOR specific activity on $PtRhSnO_2$/C was much higher than $PtSnO_2$/C and PtRu/C catalysts. The onset potential of EOR on $PtRhSnO_2$/C negatively shifted 180 mV (0.330–0.150 V versus SHE) compared with PtRu/C, as shown in Figure 4.2b. The potential-dependent peak near 2342 cm^{-1} for the signature peak asymmetric stretch vibration of CO_2 appears at 0.78 V on Pt(111) electrode, but shifts to above 0.30 V on $RhSnO_2$/Pt(111) electrode, indicating cleavage of the C−C bond in ethanol, as shown in Figure 4.2c and d. Based on DFT calculations, the dehydrogenation (of β-H) and C−C breakage steps (16 and 17) are of critical importance for achieving complete decomposition and oxidation of ethanol.

$$^*CH_3CH_2OH \rightarrow ^*CH_3CH_2O + H^* \tag{4.15}$$

$$\rightarrow ^*CH_2CH_2O + 2H^* \tag{4.16}$$

$$\rightarrow ^*CH_2 + ^*CH_2O + 2H^* \tag{4.17}$$

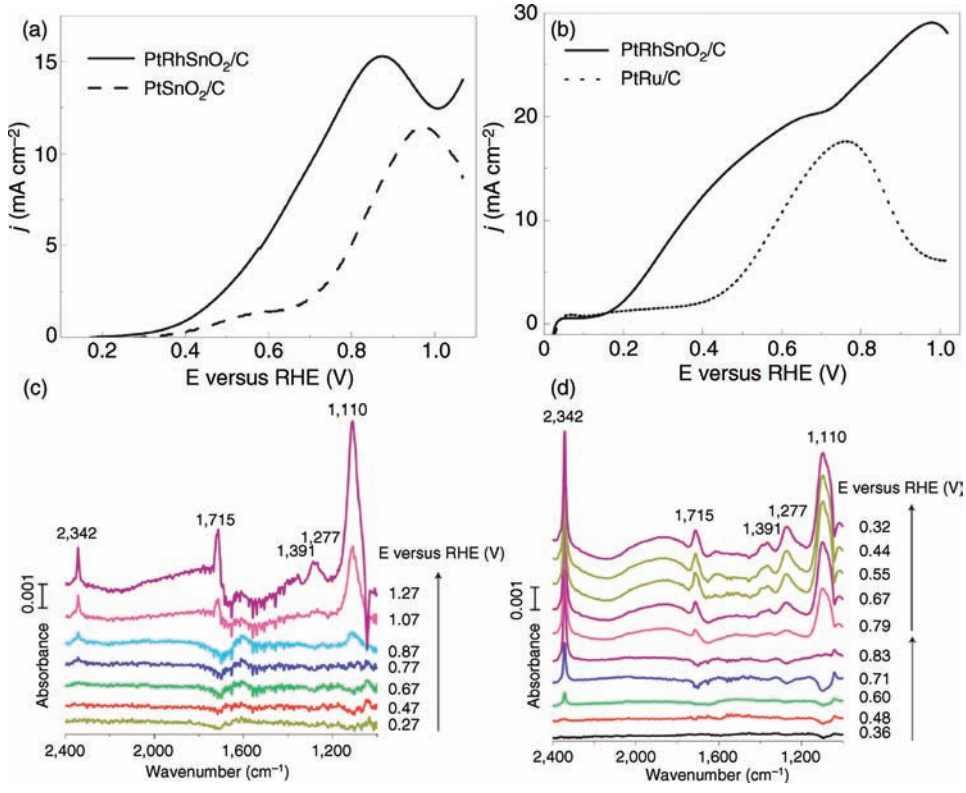

Figure 4.2 Current–potential curves comparing the activity of $PtRhSnO_2/C$ with that of several other catalysts for ethanol oxidation. Electrocatalyst compositions – $PtRhSnO_2/C$: 30 nmol Pt, 8 nmol Rh, and 60 nmol SnO_2; $PtSnO_2/C$: 30 nmol Pt and 60 nmol SnO_2 (a); $PtRhSnO_2/C$: 25 nmol Pt, 5 nmol Rh, and 20 nmol SnO_2; PtRu/C: 25 nmol Pt and 25 nmol Ru. (b) 0.1 M $HClO_4$+ 0.2 M ethanol, 50 mVs. *In situ* IRRAS spectra recorded during ethanol electrooxidation on the Pt(111) electrode (c), and $PtRhSnO_2/C$ in 0.1 M $HClO_4$ + 0.2 M ethanol solution (d) [71].

Ethanol decomposition on $RhPt/SnO_2$ occurs through an oxametallacyclic conformation ($-CH_2CHO$). The two steps, Equations 4.16 and 4.17, can be achieved by incorporating the element Rh with more lying-d band, especially when it is alloyed with Pt.

4.3.3
Anion Exchange Membrane-Based Direct Ethanol Fuel Cells (AEM-DEFCs)

The kinetics of both oxygen reduction and alcohol oxidation can be more significantly improved in a high-pH electrolyte than in a low-pH one, due to enhanced ion transport and facile charge transfer in alkali [72]. The anion exchange membrane direct ethanol fuel cells build upon AEM electrolyte and are directly fed with ethanol fuel. At the anode, the ethanol reacts with OH^- to produce CO_2 (complete oxidation), while at the cathode, oxygen reacts with H_2O and

electrons to yield OH^-. The anode, cathode, and overall reactions and their theoretical potentials are shown in Equations 4.18–4.20.

$$C_2H_5OH + 12OH^- \rightarrow 2CO_2 + 9H_2O + 12e^- \quad -0.75\,\text{V versus SHE} \quad \text{(anode)} \tag{4.18}$$

$$3O_2 + 6H_2O + 12e^- \rightarrow 12\,OH^- \quad +0.40\,\text{V versus SHE} \quad \text{(cathode)} \tag{4.19}$$

$$C_2H_5OH + 3O_2 \rightarrow 2CO_2 + 3H_2O \quad +1.15\,\text{V} \quad \text{(overall)} \tag{4.20}$$

The current AEMs are mainly based on quaternary ammonium hydroxide (QAOH) polymers [73]. They have demonstrated good thermal and chemical stability. The OH^- conductivity of a commercial AEM, such as Tokuyama A201, is as high as $38\,\text{mS}\,\text{cm}^{-1}$ [74]. These AEMs can be operated at 80 °C without structural changes. Under such low-temperature operations, undesirable decomposition of alcohol does not occur. Serious problems traditionally associated with electrolyte carbonation for liquid alkaline fuel cells can be overcome using a solid AEM electrolyte. There are no mobile cations, that is, K^+, in AEMs, so it is not easy to form precipitations (i.e., K_2CO_3) that block or destroy an electrolyte and alleviate all cation-related issues. The anions cross from cathode to anode, thus minimizing alcohol crossover problem. The AEMFCs also have price advantages over PEMFCs due to low-cost AEM membrane (hydrocarbon polymer versus poly(perfluorosulfonic acid) PEM, that is, Nafion). Owing to a less corrosive basic working environment, inexpensive non-PGMs, such as Ag and Fe/Co–N have demonstrated very competitive oxygen reduction reaction (ORR) activity and durability and can be used as AEMFC cathode catalysts [72,75,76]. All the merits have gained anion exchange membrane a lot of research attention in recent years.

4.3.4
Anode Catalysts for AEM-DEFCs

Pd has demonstrated the highest EOR activity in high-pH media among all known single-metal catalysts [5,7]. Pd is more abundant on the Earth's crust: 200 times higher than Pt (0.6 versus 0.003 ppb). Pd has a lower price than Pt. The EOR activity on Pd highly depends on pH [77,78]. Liang *et al.* suggested an EOR mechanism in high-pH media by using CV study [79]. They showed that the α-C is first activated on a Pd surface to dehydrate 2 H atoms, and to break O−H, "ethoxi" ($-CH_3CO$) forms. Ethoxi reacts with adsorbed −OH to produce acetate, this is the rate-determining step. A subtle balance between the ethanol and OH^- concentrations is required for high oxidation activity because the prevalence of either species in solution may hinder the necessary adsorption of both species, thus resulting in a lower EOR activity.

$$Pd + OH^- \rightarrow Pd - (OH)_{ads} + e^- \tag{4.21}$$

$$Pd - (CH_3CH_2OH)_{ads} + 3OH^- \rightarrow Pd - (CH_3CO)_{ads} + 3H_2O + 3e^- \tag{4.22}$$

$$Pd - (CH_3CO)_{ads} + Pd - (OH)_{ads} \rightarrow Pd - (CH_3COOH)_{ads} + Pd \tag{4.23}$$

DFT calculations on model Pd clusters have shown that dehydrogenation hardly occurs without the assistance of OH^-. Both α-C and H from the hydroxyl taking part in the ethanol oxidation are facile in the presence of OH^-, leading to the formation of acetaldehyde [78]. However, its oxidation peak has not been observed in the CV scan.

Binary Pd-M (M = Ru, Au, Sn, Cu, etc.) catalysts have been investigated and they demonstrated improved EOR activity. Chen *et al.* found that Pd–Ru shows higher activity toward methanol, ethanol, and ethylene glycol than Pd, the optimum composition being 1 : 1 [80]. PdAu and PdSn catalysts show better tolerance to poisoning species than Pt catalyst [81]. The effects of addition of various oxides (NiO, CeO_2, etc.) to carbon-supported Pd have been studied. Among them, NiO showed the highest peak current density. The possible function of oxide is because OH_{ads} species could be easily formed on the surface of oxide, the formation of OH_{ads} can assist transformation of CO-like poisoning intermediates on the Pd surface to CO_2 or other products [82]. It is interesting to note that ternary metal Pd–Ni–Zn catalysts demonstrated the highest EOR activity (its specific activity in half-cell test is $>3600\,A\,g_{Pd}^{-1}$) and excellent reaction stability [5,83,84]. The Pd-based catalysts can accelerate the EOR kinetics, but it is difficult to break the C−C bond in high-pH media. The products are exclusively carboxylates, especially for primary alcohols, that is, ethanol and isopropanol [85]. Although polyols (i.e., glycerol) may undergo C−C bond scission to form carbonate, it is still a minor reaction path, the major products being various carbohydrates [86,87].

To date, AEM-DEFCs have exhibited higher performance than PEM-DEFCs [5]. For example, an active AEM-DEFC with the Pd–Ni–Zn/C anode catalyst and Fe–Co–N/C cathode catalyst (from Acta) shows a peak power density of 200 mW cm^{-2} at 80 °C and 2 atm O_2 back pressure [83]. For PEM-DAFC, the higher alcohols, such as ethanol, ethylene glycol, and glycerol, are difficult to be oxidized even on Pt and Pt-based catalysts, unless the temperature is increased to >130 °C. The state-of-the-art PEM-DEFC with a PtSn anode catalyst has a peak power density of 50–70 mW cm^{-2} [60,64]. However, current AEM-DEFCs need liquid base mixed with alcohol fuel to provide sufficient OH^- for improving its reaction kinetics. The development of more effective anion exchange ionomer, construction of ordered electrode architectures, and examination of long-term reaction stability are the necessary research tasks for developing efficient and durable AEM-DEFCs.

4.4
Anode Catalysts for Direct Polyol Fuel Cells (Ethylene Glycol, Glycerol): Cogenerate Electricity and Valuable Chemicals Based on Anion Exchange Membrane Platform

4.4.1
Overview of Electrooxidation of Polyols

It has been known that the catalyst activity toward alcohol oxidation reaction can be significantly enhanced in alkaline electrolyte [2,88]. A recent study by Koper

and coworkers shows that the first deprotonation step in alcohol oxidation is a base-catalyzed step, and the second deprotonation depends on the ability of the electrode materials (i.e., Au or Pt) to abstract the H_β [87]. Theoretical DFT calculations further show that the adsorbed OH species are essential to accelerate many steps in alcohol oxidation, that is, the activation energy of the first deprotonation step in the absence of OH^- is as high as 204, 116 kJ mol^{-1} on Au and Pt catalysts, respectively, while it drops one order of magnitude (22 and 18 kJ mol^{-1} on Au and Pt) with assistance of adsorbed OH^- [89]. These works indicate that the base catalysis is the main driver behind the high oxidation activity of alcohols in alkaline electrolyte, but not the catalyst interaction with hydroxide.

Due to the enhanced oxidation kinetics in high-pH media, anion exchange membrane fuel cells using biomass-derived alcohol fuels (e.g., ethanol and glycerol) have recently attracted increasing attention. Accumulated evidences have shown that breaking C−C bond of C_{2+} alcohol on metal catalysts at low temperatures is very difficult, especially in high-pH media [5]. For example, the main products of ethanol oxidation are acetaldehyde and acetic acid (or acetate). This lowers the Faradic efficiency to 17–33% for direct ethanol fuel cells [6]. The use of polyol fuels can be an interesting alternative, because in the polyols, each carbon has a hydroxyl (−OH) group that can be fully oxidized to carbonyl (−CO) or carboxyl (−COOH) group; therefore, more electrons are generated even without breaking C−C bonds, and the fuel cell's Faradic efficiency improves. In addition, ethylene glycol and glycerol have competitive energy densities (5.2 and 5.0 kWh kg^{-1} for ethylene glycol and glycerol, respectively, versus 6.1 and 8.0 kWh kg^{-1} for methanol and ethanol, respectively), and they are nonflammable and nontoxic fuels.

The complete oxidation of two hydroxyl groups of ethylene glycol to oxalate without breaking C−C bond is as follows, and the Faradic efficiency is 80%.

$$CH_2OH - CH_2OH + 14OH^- \rightarrow 2{CO_3}^{2-} + 10H_2O + 10e^- \tag{4.24}$$

$$CH_2OH - CH_2OH + 10\,OH^- \rightarrow (COO - COO)^{2-} + 8H_2O + 8e^- \tag{4.25}$$

The complete oxidation of three hydroxyl groups of glycerol to mesoxalate without breaking two C−C bonds is as follows, and the Faradic efficiency is 71.5%.

$$CH_2OH - CHOH - CH_2OH + 20\,OH^- \rightarrow 3{CO_3}^{2-} + 14H_2O + 14e^- \tag{4.26}$$

$$CH_2OH - CHOH - CH_2OH + 12\,OH^- \rightarrow (COO - CO - COO)^{2-} + 10H_2O + 10e^- \tag{4.27}$$

In addition, incomplete oxidation of polyols leads to production of higher valued chemicals, such as dihydroacetone, which is a valuable tanning agent, hydroxypyruvic acid, which is a flavor component and a possible starting material for DL-serine synthesis, and tartronic and mesoxalic acids, which are important intermediates for novel polymer and pharmaceutical synthesis. Therefore, research on cogeneration of electricity and higher valued chemicals from polyols

based on anion exchange membrane fuel cell platform will not only be attractive for developing electrochemical power sources but will also help to open new routes for conversion and utilization of biomass resources.

4.4.2
Reaction Mechanisms and Catalysts for Ethylene Glycol Electrooxidation

The oxidation of EG is more complex than that of ethanol due to its two adjacent hydroxyl groups. The investigation into EG electrooxidation in alkaline media started from the mid-1970s. Since the complete oxidation of EG needs up to 10 electrons, various reactive species and reaction intermediates could be produced through several consecutive and parallel steps. Figure 4.3 illustrates the general reaction scheme for electrooxidation of EG [5]. Compounds in boxes have been detected in anode compartment of DEFCs using HPLC, among them glyoxylic acid was in trace amount over $Pt_{0.45}Pd_{0.45}Bi_{0.1}/C$ catalyst at 0.58 V for 360 min [90]. The compounds in circles have been exclusively detected in half cells using IR spectroscopy, and they are the reaction intermediates including glycolaldehyde and glyoxal. There are two paths for EG oxidation: poisoning and nonpoisoning paths. The nonpoisoning path stops at oxalate, because oxalate is very slowly oxidized on electrocatalysts, especially Pd surface. Oxalate is not a main product and it comes from further oxidation of glycolate (glycolic acid) or glycoxalate (glyoxalic acid) depending on pH. The poisoning path leads to the production of C_1 products, that is, carbonate, due to C–C bond scission in the process of further oxidation of glycolate. The applied potential plays a key role in

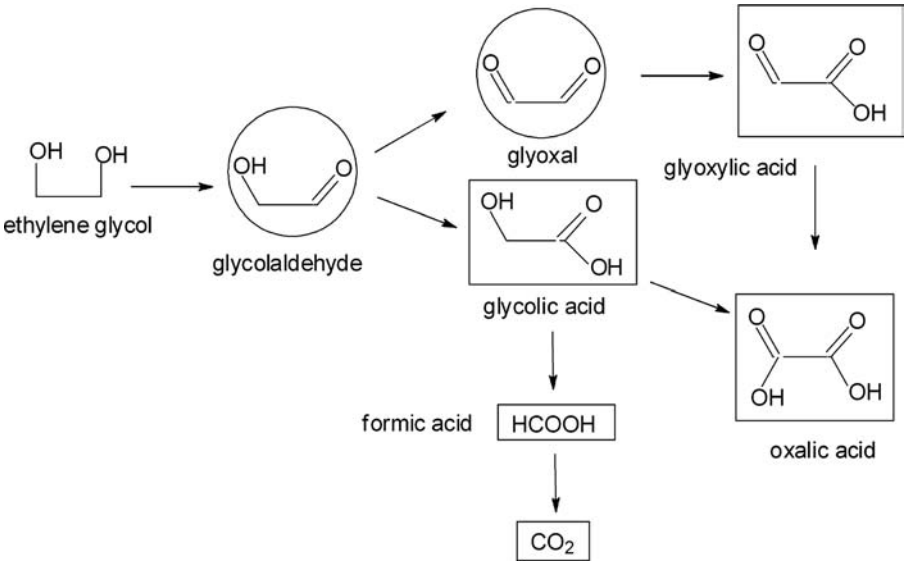

Figure 4.3 Proposed mechanism for ethylene glycol oxidation [5].

C−C bond cleavage: no C−C bond cleavage occurs at <400 mV over Pt catalyst, while the C−C bond of EG was cleaved in EG oxidation at 500 mV, which led to CO poisoning [91].

The EG electrooxidation kinetics and product distribution are quite different over Pt and Au. Cyclic voltammetry shows that the onset potential is more positive, but the peak current is larger on Au than on Pt, which indicates quite different reaction pathways. Weaver group studied the EG electrooxidation pathways in alkaline electrolytes on Pt and Au. They found that the Au featured the successive formation of partially oxidized C_2 solution-phase species *en route* to oxalate and carbonate production, while Pt was able to oxidize EG to carbonate through a sequence of chemisorbed (rather than solution-phase) intermediates [92]. Au is a very good catalyst for electrooxidation of aldehydes and alcohols in high-pH media. The electrooxidation of EG on Pd in alkaline media does not diverge that much compared with that on Pt: glycolate, oxylate, and carbonate seem to form at the same potential with an increase of oxalate and carbonate formation at the consumption of glycolate. Low pH favoring C−C bond scission is because a high OH coverage of the Pd/Pt surface is required for yielding only carboxylate products.

The activity of EG electrooxidation can be improved using binary or ternary catalysts either by alloying PGM (i.e., Pt or Pd) with different metals or by modifying the PGM surface by foreign metal ad-atoms [90,93–95]. Pt-M ad-atom (M = Bi, Cd, Cu, Pb, Re, Ru, Ti) catalysts have been studied and Pb and Bi were found to be able to improve the EG oxidation current density close to diffusion-limited value, attributed to bifunctional theory of electrocatalysts. Coutanceau and coworkers studied Pt, Pt–Pd, and Pt–Pd–Bi alloy catalysts for EG oxidation in both liquid alkaline electrolytes and AEM-based direct EG fuel cells. They found that the addition of Bi could decrease the onset potential by 70 mV, while Pt–Pd–Bi does not change the onset potential but leads to enhanced current density. EG is converted to glycolic acid, oxalic acid, and formic acid on Pt/C, while no formic acid but trace amounts of glyoxalic acid were observed on PtPdBi/C. They proposed that Bi favors the adsorption of OH species and depresses the C−C bond cleavage, which is likely due to dilution of surface Pt atoms [90]. The function of Pd is to only limit the poisoning of Pt sites by changing the composition of chemisorbed species. Nanostructured Pd–(Ni–Zn)/C and Pt–(Ni–Zn–P)/C have demonstrated to be much more active than smooth Pd electrodes up to 3300 A g_{Pd}^{-1}, and have also changed the oxidation product distributions: mixture of glycolate, oxalate, and carbonate were obtained, while most glycolate yielded on Pd/C catalyst. This indicates that Pd–(Ni–Zn)/C could promote C−C bond cleavage for a more complete oxidation [5].

4.4.3 Reaction Mechanisms and Catalysts for Glycerol Electrooxidation

Glycerol can be by-produced in large amounts in the biodiesel production [10,11]. Glycerol electrooxidation has been studied for its possible use in fuel

cells. In alkaline media, Pt, Pd, and Au have demonstrated distinct behaviors to glycerol electrooxidation. Pt/C shows a 150 mV lower onset potential and higher peak current than Pd and Au, while Au has a higher onset potential but broader GOR active potential region, which is due to its high redox potential. The Pd–Au alloy (atomic ratio of Pd–Au: 0.3 : 0.7, 0.5 : 0.5) catalysts presented comparatively lower onset potential than monometal Au/C and Pd/C ones, but still higher than Pt/C [96].

The oxidation products include glyceric acid, tartronic acid, glycolic acid, formic acid, oxalic acid, CO_2, and so on, and their distributions depend on the catalyst composition and structure and operation potential (anode overpotential) [5,50,86–88,96]. For example, an AEM-DGFC with a Pd/carbon nanotube (CNT) anode catalyst provided stable current for 8.4 h, producing 3070 C and achieving 28.6% conversion. About 4 mmol of glycerol was consumed to produce 27% glycerate, 23% tartronate, 4% glycolate, 15% oxalate, 9% formate, and 22% carbonate [50]. An electrolysis cell operated at 0.1 A and 0.6–0.7 V for 15 h in 2 M KOH + 2 M glycerol produced 35% glycerate, 36% tartronate, 3% glycolate, 14% oxalate, 2.5% formate, and 12.5% carbonate [97]. Based on these results, a reaction mechanism for glycerol oxidation is proposed, as shown in Figure 4.4. The primary OH is first oxidized to produce glyceric acid, and then the other end OH is oxidized to yield tartronic acid, glycolic acid is subsequently produced due to C−C bond scission. Glycolic and formic acids are further oxidized to produce oxalic acid, and CO_2, respectively.

Recently, Kwon and Koper used a self-designed onsite sample collection and off-line HPLC analysis system to study the mechanism of glycerol electrooxidation on Pt and Au electrodes [86]. They found a strong correlation between applied potential, catalyst (Pt and Au), and oxidation product distribution. On the Pt electrode, only glyceric acid was examined at relatively low potential, that is, <0.4 V (versus RHE), in 0.1 M NaOH + 0.1 M glycerol at 25 °C. Beyond this potential, glycolic acid and formic acid are produced due to C−C bond breaking. As the potential increases to ~0.5 V, tartronic acid and oxalic acid were examined. On the Au electrode, the onset potential of glycerol oxidation (at 0.65 V) is much higher than that of Pt. The glyceric acid is the only product under potential of ~ <0.8 V, while glycolic acid and formic acid were detected at a scan

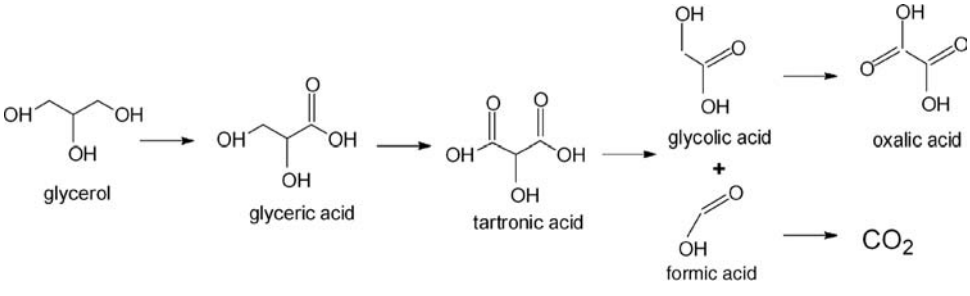

Figure 4.4 Proposed mechanism of glycerol oxidation on Pd catalysts. Adapted from Ref. [50].

potential of >0.8 V. No tartronic acid and oxalic acid were observed throughout the potential range of 1–1.8 V. This approach enables the monitoring of soluble reaction products during voltammetry with HPLC and allows new insights into mechanisms of complex multistep electrode reactions.

Controlled partial (selective) oxidation of glycerol using molecular oxygen in an aqueous-phase heterogeneous catalytic system under moderate conditions (i.e., 30–80 °C, 3–10 bar) represents a very attractive process for its low environmental impact, especially when compared with current stoichiometric oxidations; therefore, they have been extensively studied in recent years [89,98–105]. It was found that precious metals, such as Pt, Pd, Rh, and Au, are active, selective, and stable catalysts. The partial oxidation of glycerol can selectively produce value-added products. It has been found that in low-pH media, DHA can be produced with a selectivity of 35% on PtBi catalysts, while in high-pH media, the primary OH will be preferentially oxidized, and diverse products, such as C_3 acid (glyceric acid, tartronic acid), C_2 acids (glycolic acid, oxalic acid), and C_1 acid (formic acid) are produced. In heterogeneous catalysis, catalyst size and structure, the support (C or oxides), reaction conditions (i.e., temperature, O_2 pressure, ratio of catalyst to glycerol), and oxidant (O_2 or H_2O_2) are found to be able to influence the catalyst selectivity. Au is unique in heterogeneous catalytic oxidation of glycerol: The TOF is close to zero (no reaction) in the absence of a base, but a 100% selectivity to glyceric acid can be obtained at a glycerol conversion of 56% in an optimized high-pH environment [106,107]. High selectivity of glycolic acid can be achieved using H_2O_2 as oxidant. The identified electrocatalytic oxidation pathways are compared with reported heterogeneous catalytic oxidation pathways, as shown in Figure 4.5. More experimental and theoretical research efforts are needed to compare the heterogeneous catalytic oxidation and electrocatalytic oxidation of polyols, and may lead to the development of novel electrocatalysts that can efficiently cogenerate higher valued chemicals and electricity.

The AEM-DGFCs have demonstrated encouraging performance. For example, an AEM-DGFC with Pd–Ni–Zn/C anode and Fe–Co–N/C cathode catalysts have shown a maximum power density of 120 mW cm^{-2}, which is competitive to PEM-based DMFCs and two to three orders of magnitude higher than current biofuel cell with glycerol fuel (normally <1 mW cm^{-2}) [5]. Higher polyols than EG and glycerol, such as erythritol and xylitol, have been used as fuels in AEM-DAFCs with PtRu/C anode catalyst [108]. They showed lower performances than the AEM-DAFCs with EG and glycerol fuels. The reaction products have not been carefully examined and detailed mechanisms are required to be understood.

4.5 Synthetic Methods of Metal Electrocatalysts

High-performance practical electrocatalysts are essential to enhancing electrooxidation of alcohols for direct alcohol fuel cells. The overall electrocatalytic

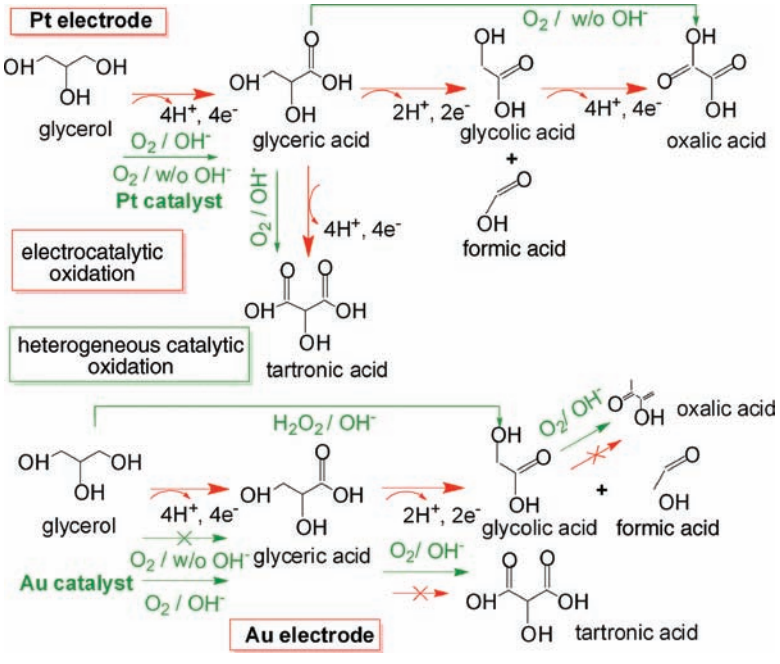

Figure 4.5 The proposed glycerol electrooxidation pathways using online collection and off-line HPLC analysis (marked in red arrows) (adapted from Ref. [87]), and reported heterogeneous catalytic oxidation of glycerol pathways (marked in green arrows) (adapted from Ref. [89]).

functions were found to be determined by local electronic property of the surface metal (d-band shift, electronic effects) [109], availability of presenting special geographic plane/facet (geometric effects) [110,111], and surface arrangements of different metals (ensemble effects) [112]. Research on single-crystal catalysts combined with theoretical calculations (e.g., DFT) have been extensively conducted in the past decades, and have provided valuable insights into the relationships of structure–catalytic functions [110,113]. For example, it was found that the overpotential for CO oxidation is lowered in the sequence of Pt (111) < Pt (554) < Pt (553), and the peak potential difference between Pt(553) and Pt(111) was as high as 0.17 V [114]. A Pt(111)skin-Ni(111) catalyst can exhibit over 90 times higher oxygen reduction reaction activity due to loose OH^- coverage on Pt skin with the modified electronic structure (optimized d-band center shift) [109,115]. However, it is still a big challenge to accurately synthesize real-world catalysts mimicking the single-crystal structures. The crucial considerations for synthesizing practical catalysts include control of the particle size, size distribution, shape (crystallographic facet), electronic structure (i.e., core–shell), nominal composition, surface composition, ensemble arrangements, alloying degree, oxide content of catalytic materials, and so on [116–118]. The long-term stability of metal catalyst and support in hostile electrochemical

environments is another practical concern [119]. The preparation method thus becomes a key factor determining the activity, selectivity, and stability of electrocatalysts.

The synthesis of real-world metal catalysts can be generally classified into "top-down" physical (from macroscale to nano dimensions) routes and "bottom-up" chemical (from molecular/atomic scale to nanoscale) routes [120]. The physical routes proceed with atomization of metals in a vacuum by thermal evaporation or sputtering, and so on [121–123]. The metal catalysts prepared by physical methods have low contaminations, and can be applied to fundamental studies. However, physical methods lacks of control over the size, size distribution, and shape of metallic particles. In contrast to physical methods, chemical methods are more flexible to precisely control the particle size, shape, and structure [124]. Recently, wet chemical synthesis approaches have emerged as one of the most promising methods to accurately control size, shape, structure, and surface facets of metallic nanostructures [118,124–140]; thus, they hold great potential for serving as high-performance catalysts. A typical wet chemical synthesis involves chemical reduction of dissoluble metal precursors in aqueous or organic phase to nucleus, controlled growth to the finally desired metal nanoparticles in the presence/absence of stabilizing agents and deposition on appropriate carbon supports. Despite the great progress in electrochemical approaches (i.e., underpotential deposition) to accurate synthesis of core–shell (skin layer) metal nanoparticles, the following section focuses only on recent advances in chemical reduction synthesis of carbon-supported electrocatalysts [141,142].

4.5.1 Impregnation Method

Impregnation method involves soaking up of a dissolved metal precursor into the pores of carbon support, and subsequently reducing the precursor into metal nanoparticles using reducing agent such as HCHO, HCOONa, $NaBH_4$, NH_2NH_2, H_2, and so on at optimized conditions [143–158]. Since the nucleation formation and particle growth are mainly confined within the carbon-support pores, the morphology of the porous substrate and the pore size distribution play a key role in terms of penetration and wetting of the precursor and also providing confinement for nanoparticle growth. In addition, the reduction kinetics and mass transfer of reducing agent also affect the number of nucleus and nucleation rate, thus controlling the particle size and particle size distribution. In order to achieve uniform dispersion of metal particles on carbon support, ethanol or isopropanol can be employed as solvent, and surface oxidation treatment of carbon support could also improve hosting metal nanoparticles. Under optimized synthesis conditions, the particle size prepared by the impregnation method can be controlled within 10 nm. The impregnation method is simple and easy to scale-up; therefore, it has been the most common method used for electrocatalyst preparation over the years. The major drawback is the lack of precise control of particle size, except when the porous substrate has a narrow

pore size distribution, that is, in highly ordered mesoporous carbon (OMC) [147]. In addition, it is hard to regulate the shape and structure of catalysts using the impregnation method. Employing an organic molecule containing two metals, such as Pt and Ru as precursor, represents a significant progress in the impregnation technique. Lukehart and coworkers synthesized (η-C_2H_4) (Cl) Pt(μ-Cl) (2)Ru(Cl) (η(3): η(3)-2,7-dimethyloctadienediyl) molecule and impregnated it onto XC-72R carbon black, and after a heat treatment under appropriate gas atmosphere, PtRu/C 16 wt% and PtRu/C 50 wt% catalysts were obtained with small particle size (3.4 and 5.0 nm, respectively) and good Pt–Ru alloy structures [146]. Although the PtRu/C catalysts demonstrated higher methanol oxidation activity than commercial PtRu/C competitors, the extra complex synthesis steps may not be suitable for a large-scale synthesis.

4.5.2 Colloidal Method

The colloid method is a widely adopted method for preparing metallic nanoparticles with precisely controlled size, shapes, and structures [125–135,137–141]. This method includes preparation of metallic colloids first and subsequent deposition on carbon support. One crucial approach is to prevent colloid aggregations using stabilizing agents, which include polymer, copolymer, surfactants, ligands, solvents, long-chain alcohols, organometallics, and so on. Effectively separating and controlling the nucleation and particle growth steps is essential for regulating the colloid size. Narrow size distributions are usually achieved either by steric hindrance of organic molecules on the metal surface or by electrostatic stabilization between nanoparticles. Watanabe *et al.* invented an elegant oxide colloid route to prepare PtRu/C. They first prepared colloidal PtRu oxides in aqueous phase with strict control of pH during adding reaction agents, and then reduced the oxide colloids by bubbling H_2 to obtain high-dispersion PtRu/C with a small particle size (2–3 nm) [159]. Bönnemann and Richards developed a delicate organic-phase reduction route to accurately control metal catalyst particle size and size distribution. NR_4BR_3H was used to reduce organic metal precursors in THF [130]. Binary and ternary catalysts such as PtRu/C, PtRuSn/C, PtRuW/C, and PtRuMo/C have been prepared through the "Bönnemann" method and showed higher performance than commercial PtRu/C catalyst [48,160].

4.5.2.1 Polyol Method

Polyol synthesis has been extensively studied for preparation of monometallic and multimetallic colloids in a polyol or diol (generally ethylene glycol), which serves as both solvent and temperature-dependent reducing agent (Figure 4.6) [126,133,139,161–164]. The presence of polyvinylpyrrolidone (PVP) can help control the particle size, shape, and structures. The key process of this method involves the reduction of inorganic precursors at an elevated temperature, sometimes close to the boiling point of polyol. It is found that at higher reduction

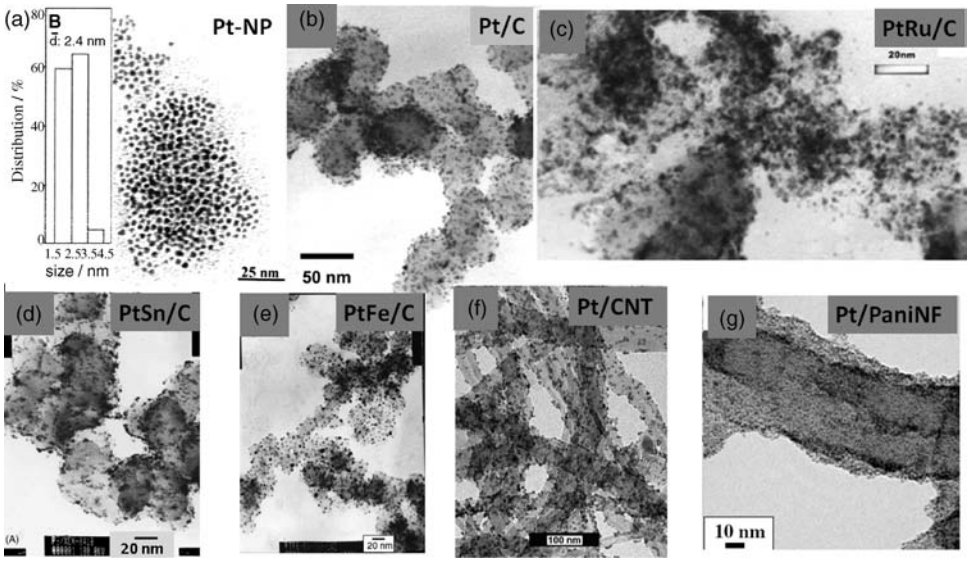

Figure 4.6 Pt and Pt-based electrocatalysts synthesized using polyol method (in the absence of PVP). (a) Pt nanoparticle ($D = 2.4$ nm [165]. (b) Pt/C (40 wt%, $D = 2.9$ nm [168]. (c) PtRu/C (20 Pt wt %, $D = 1.9$ nm [60]. (d) PtSn/C (20 Pt wt %, $D = 1.9$ nm [62]. (e) PtFe/C (20 Pt wt %, $D = 3.4$ nm [173]. (f) Pt/CNTs (30 wt%, $D = 4.46$ nm [174]. (g) Pt/polyaniline nanofibers (PaniNF, 30 wt%, $D = 2.1$ nm [176].

rates, the growth process leads to the production of thermodynamic-favored shape, while at low reduction rates, the nucleation and growth will be kinetically controlled and the shape of final products deviate from thermodynamic-favored shapes. Therefore, precise size and shape control can be achieved through rationally tuning the reaction kinetics, particularly at the seeding stage. Pt nanostructures, such as nanodendrites [139], nanorods, nanobars [152], and so on, can be accurately prepared through this method. However, the presence of stabilizers may cause intrinsic catalytic activity loss, and the postprocess for removal of stabilizers may lead to catalyst particle aggregation or shape/structure changes.

Polyol synthesis method in the absence of PVP was reported by Wang group to prepare homogeneous Pt, Rh, and Ru colloids with an average particle size of 2–4 nm [165]. Later, supported noble metal or noble metal/transition metal nanoparticles were prepared [60–65,166–179]. Xin and coworkers synthesized carbon-supported Pt, PtRu, PtPd, PtIr, PtSn, PtW, and PtFe catalysts with a sharp particle size distribution of 2–5 nm [60–65,166,168,170–173,175,177]. This method is simple and very easy to scale up. The inorganic compounds such as H_2PtCl_6, $RuCl_3$, $PdCl_2$, $SnCl_2$, $FeCl_2$, and so on served as metal precursors. The water content in the synthesis system was found to be able to control the particle size and size distribution. The reduction was conducted in an alkaline environment at 135–150 °C for 3–4 h, and the pH had to be adjusted back to 2–3 to separate the metal colloids from solvent and deposit them onto carbon support. Good alloy structures could be obtained through this method. It is very

attractive for large-scale synthesis because of the simple procedures and low material cost. However, it has to some extent failed for the synthesis of noble metal/transition metal alloy catalysts. Because EG is a weak reducing agent, transitional metal could not be fully reduced; therefore, its content is low in the final bimetallic catalysts. That is, the Fe content in the resulted PtFe/C catalyst was detected only 1/3–1/4 of its setting value [173].

4.5.2.2 Organic-Phase Method

In 2000, Sun et al researchers at IBM reported an elegant organic-phase method to prepare Fe–Pt magnetic nanoparticles with a diameter of 4–5 nm [129,180]. This approach was quickly adopted by catalysis researchers to prepare metal catalysts [134,135,137,181–188]. In nonpolar organic solvents, precious metal and transitional metal precursors have more intimate contacts and closer redox potentials; this can facilitate formation of a homogeneous bimetal nucleus, leading to the growth of controlled bimetallic nanoparticles. In the synthesis, the transitional metal precursor can be fully reduced by injecting a strong organic reducing agent, for example, $LiBetH_3$. Different C_{18}, C_{16} surfactants (e.g., oleylamine, oleic acid, octadecene, etc.) served as stabilizers that can selectively bond on specific metal facets, thus not only protecting particles from aggregations but also guiding the metal nucleus to grow into desired shapes (i.e., nanowires, nanorods, and nanoleaves) [134,184,186,188] and structures (e.g., core–shell) [135].

Figure 4.7a briefly illustrates the overall synthesis scheme. Sun *et al.* first developed this elegant synthesis route to prepare Fe–Pt magnetic materials with very narrow size distribution (4–5 nm), as shown in Figure 4.7b. Because metal precursors in the organic solvent have intimate contacts and closer redox potentials, better multimetallic catalysts can be obtained. PtCr/C, PtCo/CNT, and PdNi/C catalysts prepared through this method have very narrow size distributions of 2–5 nm and good alloy structures (Figure 4.7c–e). PdFe nanowires with

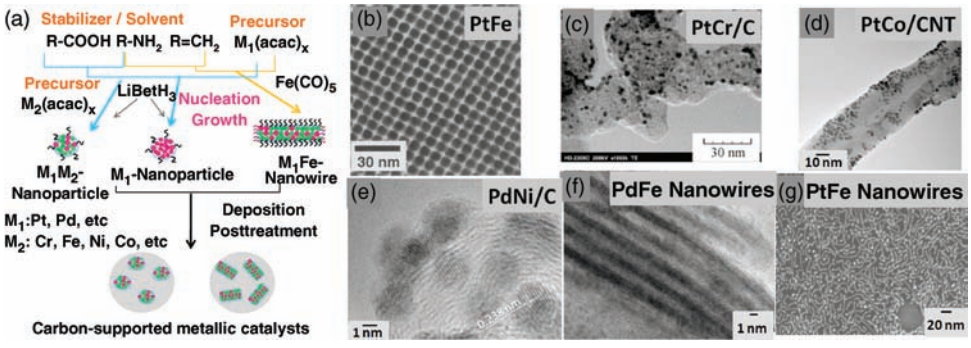

Figure 4.7 (a) Schematic illustration of the organic-phase method. Examples of catalysts prepared through this method. (b) PtFe nanoparticles [129]. (c) PtCr/C (28 wt%, $D = 2.3$ nm [187]. (d) PtCo/CNT (20 Pt wt %, $D = 2.0$ nm [180]. (e) PdNi/C (20 Pt wt %, $D = 2.4$ nm [187]. (f) PdFe nanoleaves ($D = 1.8$ nm, $L = 100$ nm [190]. (g) PtFe nanowires ($D = 2.7$ nm) [188].

a diameter of 2–3 nm and tunable length of 10–100 nm and Pd (111)-rich surface have been synthesized by changing the ratio of oleylamine and octadecene (Figure 4.7f). The PdNi/C prepared through this method has demonstrated very high reactivity to ethanol oxidation reaction in liquid alkaline electrolyte; this may be due to special interaction between surface Pd and Ni.

However, the surfactants need to be removed for electrocatalytic applications. It has been reported that surfactants could be removed under thermal treatment at a moderate temperature of 250 °C for a longer time, for example, 4 h [185]. It was also found that organic acid treatment and electrochemical tests may facilitate surfactant removal and achieve a higher reactivity [187].

4.5.3
Microemulsion Method

The microemulsion method consists of dispersion of two immiscible liquids containing reducing agent and metal precursors. It offers a unique flexibility in the simultaneous control of size and composition of mixed metal nanoparticles [189–196]. The chemical reduction of metal precursors is confined within a microemulsion, which is a tiny drop of precursor containing liquid engulfed by surfactant molecules. The microemulsion is uniformly dispersed in a continuous liquid phase, which is immiscible to the precursor-containing liquid phase. The size of the microemulsion is on the order of a few to hundreds of nanometers and is determined by the balance of surface free energy mediated by the surfactant molecules and the free energy difference arising from the immiscibility of the two liquid phases. The dispersed liquid phase is an oil, and water forms the continuous medium. The reverse microemulsion is the water-in-oil microemulsion. Since chemical steps are conducted within the microemulsion, which serves as a nanoscale reactor, a narrow particle size distribution (i.e., 2–5 nm) can thus be obtained. The introduction of a reducing agent, for example, hydrazine, $NaBH_4$, into the microemulsion is achieved by stirring. The reaction time is on the order of minutes. The size and distribution of the metal nanoparticle can be further controlled by a two-microemulsion method with the reducing agent also confined in a separate emulsion. It is possible to control the particle size by varying the water-to-surfactant molar ratio. The additional advantage is the possible synthesis of bimetal electrocatalysts on carbon support. Normally, a better alloy structure can be achieved. However, the microemulsion method cannot be used to control shape. It uses expensive surfactant molecules with extra cleaning steps and may not be suitable for large-scale synthesis.

4.5.4
Other Methods

Some unconventional synthesis techniques have been adopted in industrial catalyst manufactures. For example, 3 M researchers have developed an elegant PVD method to prepare nanostructured thin-film catalysts (NTFC) with extraordinary

activity and durability [123]. Spray conversion reaction process was successfully developed by Cabot company [197]. Droplets containing metal precursors and carbon support were first generated and thermal decomposed under controlled temperature and pressure to form uniform disperse catalyst nanoparticles on carbon. The PtRu/C catalyst has a uniform crystalline size of 2–4 nm and shows high catalytic activity, excellent durability, and reduced cost.

4.6
Carbon Nanomaterials as Anode Catalyst Support

Catalyst support is an integrated part of an electrocatalyst. Its main functions are hosting high-dispersion Pt nanoparticles from aggregation and providing continuous electric conduction paths within the three-phase boundary of the electrode. It was a milestone in the fuel cell catalyst R&D history that one order of magnitude of Pt loading in electrode could be reduced by replacing Pt black with highly disperse Pt nanoparticles supported on carbon black. Appropriate carbon support should possess excellent electric conductivity, large surface area, reasonable pore structure, and good electrochemical durability [116]. Carbon black is a widely used support for low-temperature fuel cell catalysts, and it can be produced by the oil furnace and acetylene processes. Carbon black has a good compromise between the surface area and electric conductivity. Due to its low cost and abundant availability, oil furnace carbon black, for example, Vulcan XC-72, has been broadly used for supporting electrocatalysts. It has a surface area of 200–300 $m^2 g^{-1}$, but composed of a large portion of micropores of <2 nm. Supply of reactant gas may not occur smoothly within a micropore of <2 nm. In addition, the electrochemical stability of carbon black has been reported to be a potential problem for real fuel cell operations, the loss of carbon support under high operation potential could lead to Pt agglomeration and leaching [119,198]. There is a clear need to seek more suitable catalyst support for low-temperature fuel cells. In recent decades, various carbon nanomaterials such as fullerene (C_{60}), carbon nanotubes, graphene, and mesoporous carbons have been discovered and synthesized, and further greatly promoted new research areas in nanotechnology and nanomaterials. These nanocarbons have been extensively studied as next generation of electrocatalyst support materials and many exciting progress have been made.

4.6.1
Carbon Nanotubes

Since its discovery [199], CNTs have attracted enormous attention as a novel catalyst material due to their high aspect ratio and unique electronic properties [166,167,172,174,175,177,178,199–206]. CNT is an allotrope of carbon with a cylindrical nanostructure made from curved graphite sheets. CNTs can be classified as single–walled nanotubes (SWNTs), double-walled nanotubes (DWNTs),

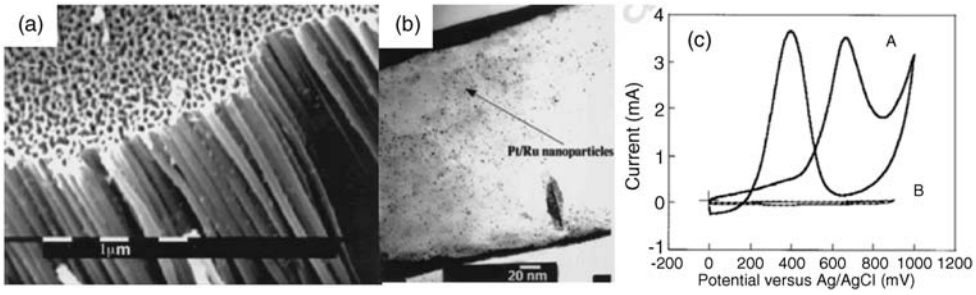

Figure 4.8 TEM images of carbon nanotubule (a) and PtRu/CNT (b), and cyclic voltammograms of methanol oxidation on A: after deposition of Pt/Ru nanoparticle, and B: before deposition of Pt/Ru nanoparticles, 2 M methanol + 1 M H_2SO_4 (c) [200].

and MWNTs. They can be prepared through arc discharge, chemical vapor deposition, laser radiation, and so on. The tube diameter ranges from 0.7to 100 nm, and tube length varies from submicrometer to centimeter. CNT is a unique 1D carbon material and possesses an excellent electric conductivity. The electric conductivity of MWNTs is 1000–2000 S cm^{-1}, which is much greater than 4–10 S cm^{-1} for carbon black XC-72. In addition, there is no micropores in CNTs compared with about 50% micropores for XC-72.

Che *et al.* first explored porous alumina template to prepare carbon nanotubule with a diameter of 200 nm and wall thickness of 20 nm (Figure 4.8). After impregnating PtRu precursors into the CNT, HF was employed to remove Al_2O_3 frames. Small and uniform PtRu nanoparticles (1.59 ± 0.3 nm) were obtained after 3 h H_2 reduction at 580 °C. The carbon nanotubule-supported PtRu nanoparticles have demonstrated very large and characteristic methanol oxidation waves in acid electrolyte [200]. Using a similar method, Rajesh *et al.* studied the methanol oxidation activity on a series of MWNTs (200 nm in diameter) and found their activity sequence is PtRu/MWNTs > Pt-WO_3/MWNTs > PtRu/XC-72 [203].

Before the synthesis of CNT-supported catalysts, it is necessary to functionalize the CNT outer wall surface with oxygenate groups in order to anchor the metal nanoparticles. Li *et al.* used a H_2SO_4–HNO_3 mixture to surface-treat MWNTs and various functional groups, such as hydroxyl (−OH), cabonyl (−CO), and carboxyl (−COOH), could be grafted on the CNT surface. They used polyol method to prepare 10 wt% Pt/MWNTs cathode catalyst for DMFC and demonstrated a 43% peak power density enhancement [186,202]. Liu *et al.* prepared PtRu/CNTs with a diameter of 2–6 nm using a microwave-promoted polyol synthesis approach and showed a competitive MOR activity compared with commercial PtRu/C (E-TEK) in single DMFC test [167]. Single-walled carbon nanohorn (SWNHs) is a special type of CNT prepared by Iijima. Pt and PtRu nanoparticles were deposited on the outer wall of SWNH and showed a significant enhancement in DMFC performance. The catalytic activity improvements were attributed to high electric conductivity (low internal resistance), high

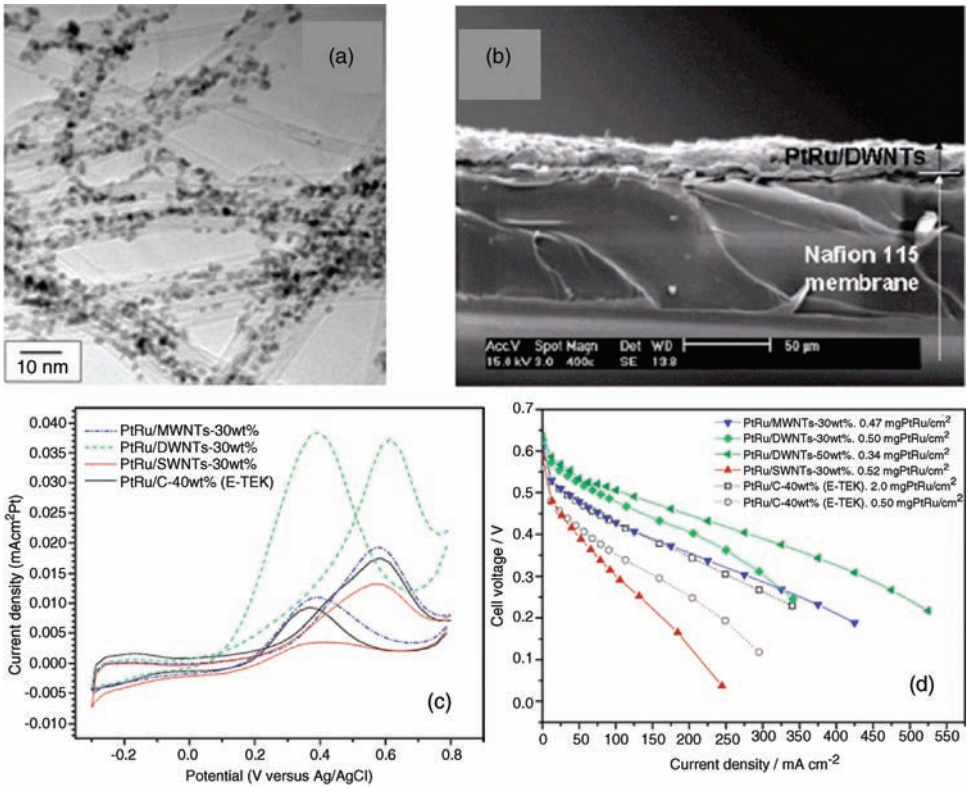

Figure 4.9 (a) TEM image of PtRu/DWNTs (50 wt%). (b) SEM image of PtRu/DWNTs thin film. (c) Polarization curve of methanol oxidation in 0.5 M H_2SO_4 + 0.5 M methanol on PtRu/CNT catalysts. (d) Single DMFC with PtRu/CNTs anode catalysts [177].

purity (i.e., low sulfur content in CNTs), and a thinner catalyst layer thickness. Recently, Li *et al.* compared three types of CNT (MWNT, DWNT, and SWNT)-supported PtRu catalysts with similar PtRu particle size (2–5 nm), and achieved very different MOR activities (Figure 4.9). PtRu/DWNTs show the best MOR activity. It can reduce precious metal loading by 75%, while still obtain a 68% power density enhancement, which was attributed to its "pure" metallic property (unlike SWNTs: a mixture of semiconductor and conductor) and a special metal support interaction [177]. Detailed investigations are needed to explain this extraordinary benefit acquired from small-diameter carbon nanotubes.

In order to improve the catalyst utilization and reactant mass transport, some research efforts have been made to develop techniques that enable to directly grow CNTs onto gas diffusion layer to obtain ordered electrode structures. Sun *et al.* directly grew CNTs on Co-Ni catalysts previously deposited on a carbon paper, and then supported small Pt nanoparticles (1.2 nm) through ion exchange method [204]. Yan and coworkers used underpotential deposition method to deposit Pt nanoparticles on CNTs, which were directly grew on carbon paper

substrate using a catalytic chemical deposition approach [205]. Both the CNT-based electrodes showed improved performance compared with Pt/C catalyst-based electrodes. Yan and coworkers further developed a filtration method to make ordered CNT-based electrode. In detail, they employed hydrophilic Nylon filter to facilitate formation of a hydrophobic CNT catalyst thin film. Pt/MWNTs thin-film electrode-based MEA demonstrated excellent single fuel cell performance in mass transport-controlled region, which indicated a better gas diffusion was achieved inside the ordered electrode [175].

Due to their high graphite structure, the CNTs have shown greater electrochemical durability than carbon black. The measured corrosion current for carbon black was 0.5 mA mg^{-1}, which is higher than that for MWNTs (0.2 mA mg^{-1}). The electrochemical surface area of Pt/MWNTs dropped 25% after a durability test under a constant potential of 0.9 V in 0.5 M H_2SO_4 at 60 °C for 170 h, while that of Pt/CB had dropped 80%. The average particle size of Pt/MWNTs grew from 2.8 nm to 3.0 nm, while that for Pt/CB grew from 2.5 to 5.0 nm [207]. Higher electrochemical stability makes CNTs very attractive for fuel cell catalyst supports.

4.6.2
Carbon Nanofibers

Carbon nanofiber (CNF) is an important 1D nanocarbon, which has also been extensively studied as electrocatalyst support [146,151,203,208–212]. Compared with expensive CNT, CNFs are cheap, attributed to their large-scale chemical vapor deposition manufacture route. CNFs can be made in different forms, such as platelet, ribbon, and herringbone. Bessel *et al.* employed impregnation method to prepare Pt/CNFs with small particle size. It was interesting to find Pt nanoparticles look like plates, which suggested a strong metal–support interaction. Five wt% Pt/CNFs showed a similar activity of methanol oxidation as 30 wt% Pt/CB [208]. Lukehart and coworkers prepared 40 wt% PtRu/CNFs with a particle size of 5–9 nm, and demonstrated a 50% MOR activity enhancement compared with unsupported PtRu catalysts [146,151]. Recently, Li *et al.* showed that CNF-based catalysts can effectively increase the Nafion content in the electrode (from 30 to 50%); this was because 1D CNFs provide continuous electric conduction paths, which could not be easily cut off by ionic conductor. This work may open up a new strategy to fabrication of high-performance fuel cell electrodes by using 1D carbon materials.

4.6.3
Ordered Mesoporous Carbons

OMCs have highly ordered mesoporous structures with very narrow pore size distributions. Uniform and small metal catalysts can be easily prepared even using impregnation method. Ordered mesoporous carbons are one type of

carbon support that have been extensively studied for direct alcohol fuel cell catalysts [147,213]. The OMC can be synthesized via nanocasting technique using ordered mesoporous silica materials as the hard template [147,213–216]. Insertion of carbon precursors within the ordered mesopores of the OMS templates, their carbonization by thermal treatment at high temperatures under inert conditions, and subsequent removal of the silica templates result in the synthesis of OMC materials. The physical and chemical properties of OMC, such as pore size, connectivity, morphology, surface functionality, electric conductivity, and thermal stability, can be well controlled by adjusting OMS template, carbon precursor, carbonation temperature, heating environment, posttreatment, and so on. Soft-templating methods (self-assembly) can also be employed to directly synthesize OMC via an organic–organic self-assembly between carbon precursors and organic templates [217–219]. The resulting OMC have a confined mesopore size, high surface area (700–2000 $m^2 g^{-1}$), and high pore volume (1–2 $cm^3 g^{-1}$). Very small Pt or PtRu nanoparticles of <3 nm can be easily controlled, simply through impregnation method, due to the OMC's large surface area and unique pore structure. The Pt/OMC cathode catalyst-based DMFC shows a 104 mW cm^{-2} at 0.45 V at 50 °C, which can reduce Pt loading by three times (from 6 to 2 mg cm^{-2}) [220]. Samsung has demonstrated a small DMFC system with 20 MEAs (25 cm^2) could deliver a power density of 80 mW cm^{-2} at 8 V using a 0.75 M methanol solution under ambient operation condition, and it can operate a Notebook for 10 h using pure 100 ml methanol.

4.6.4
Graphene Sheets

Graphene, a two-dimensional carbon material with single (or a few) atomic layer, has attracted great attention from both fundamental science and applied research [221,222]. The combination of the high surface area (theoretical value of 2630 $m^2 g^{-1}$), high conductivity, unique graphitized basal plane structure, and potential low manufacturing cost makes graphene sheets a very promising candidate for fuel cell catalyst support [223–227]. In addition, graphene nanosheets (GNS) have been found to be able to modify the properties of Pt clusters supported on them. The Pt/GNS showed four times higher current density (0.12 mA cm^{-2}) than that of Pt/CB (0.03 mA cm^{-2}). CO oxidation study indicated that Pt/GNS has a much smaller CO adsorption rate by about 40 times than that of Pt/carbon black. The Pt particles supported on GNS was smaller than 0.5 nm, which would acquire the specific electronic properties of Pt, thus modifying its catalytic activities [224]. The Pt-functionalized graphene sheets (FGS) retained 49.8% of the original electrochemical surface area, while the commercial catalyst kept only 33.6% after an electrochemical durability test. Therefore, Pt on FGSs is much more stable than commercial catalyst under electrochemical durability tests, due to its more graphite structure [223].

4.7 Future Challenges and Opportunities

Low-temperature direct alcohol fuel cells have received enormous attention for future electrochemical power sources. Anode catalyst is one of the most critical components to determine the overall DAFC performance and lifetime. Extensive research efforts have been made on understanding the relationships of structure–catalyst functions, *in situ* characterizing reaction intermediates, elucidating electrocatalytic reaction mechanisms, and thus developing novel catalytic materials. Although great progress has been made in the preparation of highly efficient fuel cell catalysts, a large-scale, accurate synthesis of fuel cell catalysts at the nano or atomic scale with high activity, durability/reliability, and stability is yet to be achieved. The synthesis methods should be cost-effective, simple, and easy to scale up. These catalysts could be heterogeneous nanoarchitectures with multiple functions supported on durable supports, or directly deposited on electrodes. Restructuring of the nanostructured catalysts (change in surface composition, facets, ensemble configuration, and electronic structures) under real electrochemical reactions often occurs and significantly influences the activity and durability; understanding the catalyst restructuring to gain deep insights into structure change–catalyst function under real electrocatalytic processes is essential before their real applications. The fast developed nanotechnology, *in situ* characterization techniques, and advanced computation capabilities have great potential to assist developing advanced catalytic materials.

In order to improve the Faradic efficiency and fuel utilization, the desired final product of alcohol oxidation is CO_2. However, breaking the C−C bonds of alcohols for direct C_{2+} alcohol fuel cells remains a great challenge, especially at low temperatures (e.g., <90 °C) and low anode overpotentials. For primary alcohol oxidation, such as ethanol oxidation, nanostructured PtRhSn/C has demonstrated a strong ability to both improve reaction kinetics and break C−C bond. Future research efforts using both combinational chemistry methods and theoretical calculations may lead to the development of efficient ternary or even quarterly PtSn-based catalysts for complete alcohol oxidation.

In another aspect, high reaction kinetics is sometimes associated with partial oxidation of alcohols. Cogeneration of electricity and higher valued chemicals from biorenewable polyols will make biofuel production more profitable and attractive. Efficient cogeneration depends on the development of highly selective electrocatalysts. The catalyst selectivity towards polyols electrooxidation is related to catalyst kind and structure, operation potential, and reaction condition [96,228–233]. Their relations should be thoroughly understood by combining experimental, analysis (e.g., spectroscopy, chromatography), and theoretical research tools. Heterogeneous catalytic processing of biorenewable compounds has made significant progress in recent years. Learning the knowledge developed from selective heterogeneous catalytic oxidation may guide the development of highly selective electrocatalytic oxidation catalysts for low-temperature alcohol fuel cells.

The oxygen reduction reaction at the cathode of a DAFC is a long-term scientific challenge. Its overpotential is over 200 mV even at the open-circuit voltage on the most active Pt catalysts. The alcohol crossover results in a short-circuit potential (extra 150–200 mV loss) at the cathode, thus seriously deteriorating the fuel cell efficiency and fuel utilization. Developing highly active low loading noble metal anode catalysts and alcohol-tolerant non-PGM cathode catalysts is in great demand for high-performance DAFCs. Since the anions cross from cathode to anode, the alcohol crossover issue can be significantly minimized through using AEMFCs. However, big disadvantages of current anion exchange membranes are their low anion conductivity and unsatisfied chemical stability (short lifetime). Liquid base, such as NaOH or KOH, has to mix with alcohol fuels to improve the local pH-surrounded catalyst sites in order to improve the DAFC performance. The penetration of carbonate salts into electrode pores will reduce reactant gas mass transfer and lead to low fuel cell performance. Development of novel polymers for high-performance anion exchange membranes should be regarded as of same important research priority as the electrocatalysts for next-generation low-temperature low/zero liquid base alcohol fuel cells.

Acknowledgments

The author would like to acknowledge the contributions of Li group members at Michigan Technological University and the support of US National Science Foundation (CBET-1032547 and CBET-1159448). The donors of the American Chemical Society Petroleum Research Fund are also acknowledged. Li thanks Dr. Zhou, Weijiang, for his fruitful discussion.

References

1 Wasmus, S. and Küver, A. (1999) Methanol oxidation and direct methanol fuel cells: a selective review. *Journal of Electroanalytical Chemistry*, **461** (1–2), 14–31.

2 Lamy, C., Belgsir, E.M., and Léger, J.M. (2001) Electrocatalytic oxidation of aliphatic alcohols: application to the direct alcohol fuel cell (DAFC). *Journal of Applied Electrochemistry*, **31** (7), 799–809.

3 Gasteiger, H.A., Kocha, S.S., Sompalli, B., and Wagner, F.T. (2005) Activity benchmarks and requirements for Pt, Pt-alloy, and non-Pt oxygen reduction catalysts for PEMFCs. *Applied Catalysis B: Environmental*, **56** (1–2), 9–35.

4 Aricò, A.S., Baglio, V., and Antonucci, V. (2009) Direct methanol fuel cells: history, status and perspectives, in *Electrocatalysis of Direct Methanol Fuel Cells: From Fundamentals to Applications* (eds. H. Liu and J. Zhang), Wiley-VCH Verlag GmbH, Weinheim, pp. 1–78.

5 Bianchini, C. and Shen, P.K. (2009) Palladium-based electrocatalysts for alcohol oxidation in half cells and in direct alcohol fuel cells. *Chemical Reviews*, **109** (9), 4183–4206.

6 Lamy, C., Coutanceau, C., and Leger, J.-M. (2009) The direct ethanol fuel cell: a challenge to convert bioethanol cleanly into electric energy, in *Catalysis for*

Sustainable Energy Production (eds P. Barbaro and C. Bianchini), Wiley-VCH Verlag GmbH, Weinheim, pp. 1–46.

7 Antolini, E. and Gonzalez, E.R. (2010) Alkaline direct alcohol fuel cells. *Journal of Power Sources*, **195** (11), 3431–3450.

8 Yu, E.H., Krewer, U., and Scott, K. (2010) Principles and materials aspects of direct alkaline alcohol fuel cells. *Energies*, **3** (8), 1499–1528.

9 U.S. DOE (2011) 2010 Annual Progress Report: DOE Hydrogen Program, in Related Information, U.S. Department of Energy.

10 Huber, G.W., Iborra, S., and Corma, A. (2006) Synthesis of transportation fuels from biomass: chemistry, catalysts, and engineering. *Chem Rev.*, **3**7 (52), 4044–4098.

11 van Santen, R.A. (2007) Renewable catalytic technologies: a perspective, in *Catalysis for Renewables: From Feedstock to Energy Production* (eds G. Centi and R. A.van Santen), Wiley-VCH Verlag GmbH, Weinheim, pp. 1–19.

12 Huber, G.W. (2008) *Breaking the Chemical and Engineering Barriers to Lignocellulosic Biofuels: Next Generation Hydrocarbon Biorefineries*, National Science Foundation, Chemical, Bioengineering, Environmental and Transport Systems Division, Washington, DC.

13 Wang, Q., Sun, G.Q., Jiang, L.H., Xin, Q., Sun, S.G., Jiang, Y.X., Chen, S.P., Jusys, Z., and Behm, R.J. (2007) Adsorption and oxidation of ethanol on colloid-based Pt/C, PtRu/C and Pt3Sn/C catalysts: *in situ* FTIR spectroscopy and on-line DEMS studies. *Physical Chemistry Chemical Physics*, **9** (21), 2686–2696.

14 Justi, E.W. and Winsel, A.W. (1955) 821 688.

15 Bagotzky, V.S. and Vassilyev, Y.B. (1967) Mechanism of electro-oxidation of methanol on the platinum electrode. *Electrochimica Acta*, **12** (9), 1323–1343.

16 Cathro, K. (1969) The oxidation of water-soluble organic fuels using platinum-tin catalysts. *Journal of Electroanalytical Chemistry and Interfacial Electrochemistry*, **16**, 1608–1611.

17 Watanabe, M. and Motoo, S. (1975) Electrocatalysis by ad-atoms: Part II. Enhancement of the oxidation of methanol on platinum by ruthenium ad-atoms. *Journal of Electroanalytical Chemistry and Interfacial Electrochemistry*, **60** (3), 267–273.

18 Janssen, M.M.P. and Moolhuysen, J. (1976) Binary systems of platinum and a second metal as oxidation catalysts for methanol fuel cells. *Electrochimica Acta*, **21** (11), 869–878.

19 Andrew, M.R., McNicol, B.D., Short, R.T., and Drury, J.S. (1977) Electrolytes for methanol-air fuel cells. I. The performance of methanol electro-oxidation catalysts in sulphuric acid and phosphoric acid electrolytes. *Journal of Applied Electrochemistry*, **7** (2), 153–160.

20 Markovic, N.M., Widelov, A., Ross, P.N., Monterio, O.R., and Brown, I.G. (1977) Electrooxidation of CO and CO/H_2 mixtures on a Pt-Sn catalyst prepared by an implantation method. *Catalysis Letters*, **43**, 161–166.

21 Beden, B., Kadirgan, F., Lamy, C., and Leger, J.M. (1981) Electrocatalytic oxidation of methanol on platinum-based binary electrodes. *Journal of Electroanalytical Chemistry and Interfacial Electrochemistry*, **127** (1–3), 75–85.

22 Shibata, M. and Motoo, S. (1985) Electrocatalysis by ad-atoms: Part XI. Enhancement of acetaldehyde oxidation by Shole control and oxygen adsorbing ad-atoms. *Journal of Electroanalytical Chemistry and Interfacial Electrochemistry*, **187** (1), 151–159.

23 Cameron, D.S., Hards, G.A., Harrison, B., and Potter, R.J. (1987) Direct methanol fuel cells. *Platinum Metals Reviews*, **31**, 173–181.

24 Aramata, A., Kodera, T., and Masuda, M. (1988) Electrooxidation of methanol on platinum bonded to the solid polymer electrolyte, Nafion. *Journal of Applied Electrochemistry*, **18** (4), 577–582.

25 Goodenough, J.B., Hamnett, A., Kennedy, B.J., Manoharan, R., and Weeks, S.A. (1988) Methanol oxidation on unsupported and carbon supported Pt + Ru anodes. *Journal of Electroanalytical*

Chemistry and Interfacial Electrochemistry, **240** (1–2), 133–145.

26 Parsons, R. and VanderNoot, T. (1988) The oxidation of small organic molecules: a survey of recent fuel cell related research. *Journal of Electroanalytical Chemistry and Interfacial Electrochemistry*, **257** (1–2), 9–45.

27 Ticanelli, E., Beery, J.G., Paffett, M.T., and Gottesfeld, S. (1989) An electrochemical, ellipsometric, and surface science investigation of the PtRu bulk alloy surface. *Journal of Electroanalytical Chemistry and Interfacial Electrochemistry*, **258** (1), 61–77.

28 Christensen, P.A., Hamnett, A., and Troughton, G.L. (1993) The role of morphology in the methanol electro-oxidation reaction. *Journal of Electroanalytical Chemistry*, **362** (1–2), 207–218.

29 Marković, N.M., Gasteiger, H.A., Ross, P.N., Jr., Jiang, X., Villegas, I., and Weaver, M.J. (1995) Electro-oxidation mechanisms of methanol and formic acid on Pt-Ru alloy surfaces. *Electrochimica Acta*, **40** (1), 91–98.

30 McBreen, J. and Mukerjee, S. (1995) *In situ* X-ray absorption studies of a Pt-Ru electrocatalyst. *Journal of the Electrochemical Society*, **142** (10), 3399–3404.

31 Ravikumar, M.K. and Shukla, A.K. (1996) Effect of methanol crossover in a liquid-feed polymer-electrolyte direct methanol fuel cell. *Journal of the Electrochemical Society*, **143** (8), 2601–2606.

32 Gurau, B., Viswanathan, R., Liu, R., Lafrenz, T.J., Ley, K.L., Smotkin, E.S., Reddington, E., Sapienza, A., Chan, B.C., Mallouk, T.E., and Sarangapani, S. (1998) Structural and electrochemical characterization of binary, ternary, and quaternary platinum alloy catalysts for methanol electro-oxidation1. *The Journal of Physical Chemistry B*, **102** (49), 9997–10003.

33 Reddington, E., Sapienza, A., Gurau, B., Viswanathan, R., Sarangapani, S., Smotkin, E.S., and Mallouk, T.E. (1998) Combinatorial electrochemistry: a highly parallel, optical screening method for discovery of better electrocatalysts. *Science*, **280** (5370), 1735–1737.

34 Sun, S.G. (1998) Studying electrocatalytic oxidation of small organic molecules with in-situ infra spectroscopy, in *Electrocatalysis (Frontiers in Electrochemistry)* (eds J. Lipkowski and P.N. Ross), Wiley-VCH Verlag GmbH, Weinheim, pp. 243–290.

35 Liu, R., Iddir, H., Fan, Q., Hou, G., Bo, A., Ley, K.L., Smotkin, E.S., Sung, Y.E., Kim, H., Thomas, S., and Wieckowski, A. (2000) Potential-dependent infrared absorption spectroscopy of adsorbed CO and X-ray photoelectron spectroscopy of arc-melted single-phase Pt, PtRu, PtOs, PtRuOs, and Ru electrodes. *The Journal of Physical Chemistry B*, **104** (15), 3518–3531.

36 Iwasita, T. (2002) Electrocatalysis of methanol oxidation. *Electrochimica Acta*, **47** (22–23), 3663–3674.

37 Piela, P., Eickes, C., Brosha, E., Garzon, F., and Zelenay, P. (2004) Ruthenium crossover in direct methanol fuel cell with Pt-Ru black anode. *Journal of the Electrochemical Society*, **151** (12), A2053–A2059.

38 Cao, D., Lu, G.Q., Wieckowski, A., Wasileski, S.A., and Neurock, M. (2005) Mechanisms of methanol decomposition on platinum: a combined experimental and *ab initio* approach. *The Journal of Physical Chemistry B*, **109** (23), 11622–11633.

39 Brockris, J.O.M. and Wroblowa, H. (1964) Activity of electrolytically deposited platinum and ruthenium by the electrooxidation of methanol. *Journal of Electroanalytical Chemistry and Interfacial Electrochemistry*, **7**, 428.

40 Petry, G.A., Podlovchenko, B.I., Frukmin, A.N., and Lal, H. (1965) The behavior of platinized-platinum and platinum-ruthenium electrodes in methanol solutions. *Journal of Electroanalytical Chemistry and Interfacial Electrochemistry*, **10**, 253.

41 Méli, G., Léger, J.M., Lamy, C., and Durand, R. (1993) Direct electrooxidation of methanol on highly dispersed platinum-based catalyst electrodes:

temperature effect. *Journal of Applied Electrochemistry*, **23** (3), 197–202.
42 Rolison, D.R., Hagans, P.L., Swider, K.E., and Long, J.W. (1999) Role of hydrous ruthenium oxide in Pt–Ru direct methanol fuel cell anode electrocatalysts: the importance of mixed electron/proton conductivity. *Langmuir*, **15** (3), 774–779.
43 Long, J.W., Stroud, R.M., Swider-Lyons, K.E., and Rolison, D.R. (2000) How to make electrocatalysts more active for direct methanol oxidation avoid PtRu bimetallic alloys!. *The Journal of Physical Chemistry B*, **104** (42), 9772–9776.
44 Rolison, D.R. (2003) Catalytic nanoarchitectures: the importance of nothing and the unimportance of periodicity. *Science*, **299** (5613), 1698–1701.
45 Ren, X., Wilson, M.S., and Gottesfeld, S. (1996) High performance direct methanol polymer electrolyte fuel cells. *Journal of the Electrochemical Society*, **143** (1), L12–L15.
46 Kim, T., Kobayashi, K., Takahashi, M., and Nagai, M. (2005) Effect of Sn in Pt-Ru-Sn ternary catalysts for CO/H_2 and methanol electrooxidation. *Chemistry Letters*, **34** (6), 798–799.
47 Page, T., Johnson, R., Hormes, J., Noding, S., and Rambabu, B. (2000) A study of methanol electro-oxidation reactions in carbon membrane electrodes and structural properties of Pt alloy electro-catalysts by EXAFS. *Journal of Electroanalytical Chemistry*, **485** (1), 34–41.
48 Park, K.-W., Choi, J.-H., Kwon, B.-K., Lee, S.-A., Sung, Y.-E., Ha, H.-Y., Hong, S.-A., Kim, H., and Wieckowski, A. (2002) Chemical and electronic effects of Ni in Pt/Ni and Pt/Ru/Ni alloy nanoparticles in methanol electrooxidation. *The Journal of Physical Chemistry B*, **106** (8), 1869–1877.
49 Antolini, E., Salgado, J.R.C., and Gonzalez, E.R. (2006) The methanol oxidation reaction on platinum alloys with the first row transition metals: the case of Pt–Co and –Ni alloy electrocatalysts for DMFCs: a short review. *Applied Catalysis B: Environmental*, **63** (1–2), 137–149.
50 Bambagioni, V., Bianchini, C., Marchionni, A., Filippi, J., Vizza, F., Teddy, J., Serp, P., and Zhiani, M. (2009) Pd and Pt–Ru anode electrocatalysts supported on multi-walled carbon nanotubes and their use in passive and active direct alcohol fuel cells with an anion-exchange membrane (alcohol=methanol, ethanol, glycerol). *Journal of Power Sources*, **190** (2), 241–251.
51 Farrell, A.E., Plevin, R.J., Turner, B.T., Jones, A.D., O'Hare, M., and Kammen, D.M. (2006) Ethanol can contribute to energy and environmental goals. *Science*, **311** (5760), 506–508.
52 Simões, F.C., dos Anjos, D.M., Vigier, F., Léger, J.M., Hahn, F., Coutanceau, C., Gonzalez, E.R., Tremiliosi-Filho, G., de Andrade, A.R., Olivi, P., and Kokoh, K.B. (2007) Electroactivity of tin modified platinum electrodes for ethanol electrooxidation. *Journal of Power Sources*, **167** (1), 1–10.
53 Iwasita, T. and Pastor, E. (1994) A DEMS and FTIR spectroscopic investigation of adsorbed ethanol on polycrystalline platinum. *Electrochimica Acta*, **39** (4), 531–537.
54 Pastor, E. and Iwasita, T. (1994) D/H exchange of ethanol at platinum electrodes. *Electrochimica Acta*, **39** (4), 547–551.
55 Perez, J.M., Beden, B., Hahn, F., Aldaz, A., and Lamy, C. (1989) "*In situ*" infrared reflectance spectroscopic study of the early stages of ethanol adsorption at a platinum electrode in acid medium. *Journal of Electroanalytical Chemistry and Interfacial Electrochemistry*, **262** (1–2), 251–261.
56 Rousseau, S., Coutanceau, C., Lamy, C., and Léger, J.M. (2006) Direct ethanol fuel cell (DEFC): electrical performances and reaction products distribution under operating conditions with different platinum-based anodes. *Journal of Power Sources*, **158** (1), 18–24.
57 Lamy, C., Lima, A., LeRhun, V., Delime, F., Coutanceau, C., and Léger, J.-M. (2002) Recent advances in the development of direct alcohol fuel cells

(DAFC). *Journal of Power Sources*, **105** (2), 283–296.

58 Lamy, C., Rousseau, S., Belgsir, E.M., Coutanceau, C., and Léger, J.M. (2004) Recent progress in the direct ethanol fuel cell: development of new platinum–tin electrocatalysts. *Electrochimica Acta*, **49** (22–23), 3901–3908.

59 Ermete, A. (2007) Catalysts for direct ethanol fuel cells. *Journal of Power Sources*, **170** (1), 1–12.

60 Zhou, W.J., Zhou, Z.H., Song, S.Q., Li, W.Z., Sun, G.Q., Tsiakaras, P., and Xin, Q. (2003) Pt based anode catalysts for direct ethanol fuel cells. *Applied Catalysis B: Environmental*, **46** (2), 273–285.

61 Zhao, X., Li, W., Jiang, L., Zhou, W., Xin, Q., Yi, B., and Sun, G. (2004) Multi-wall carbon nanotube supported Pt-Sn nanoparticles as an anode catalyst for the direct ethanol fuel cell. *Carbon*, **42** (15), 3263–3265.

62 Zhou, W.J., Li, W.Z., Song, S.Q., Zhou, Z.H., Jiang, L.H., Sun, G.Q., Xin, Q., Poulianitis, K., Kontou, S., and Tsiakaras, P. (2004) Bi- and tri-metallic Pt-based anode catalysts for direct ethanol fuel cells. *Journal of Power Sources*, **131** (1–2), 217–223.

63 Zhou, W.J., Song, S.Q., Li, W.Z., Sun, G. Q., Xin, Q., Kontou, S., Poulianitis, K., and Tsiakaras, P. (2004) Pt-based anode catalysts for direct ethanol fuel cells. *Solid State Ionics*, **175** (1–4), 797–803.

64 Zhou, W.J., Zhou, B., Li, W.Z., Zhou, Z.H., Song, S.Q., Sun, G.Q., Xin, Q., Douvartzides, S., Goula, M., and Tsiakaras, P. (2004) Performance comparison of low-temperature direct alcohol fuel cells with different anode catalysts. *Journal of Power Sources*, **126** (1–2), 16–22.

65 Zhou, W.J., Song, S.Q., Li, W.Z., Zhou, Z.H., Sun, G.Q., Xin, Q., Douvartzides, S., and Tsiakaras, P. (2005) Direct ethanol fuel cells based on PtSn anodes: the effect of Sn content on the fuel cell performance. *Journal of Power Sources*, **140** (1), 50–58.

66 Vigier, F., Coutanceau, C., Hahn, F., Belgsir, E.M., and Lamy, C. (2004) On the mechanism of ethanol electro-oxidation on Pt and PtSn catalysts: electrochemical and *in situ* IR reflectance spectroscopy studies. *Journal of Electroanalytical Chemistry*, **563** (1), 81–89.

67 Vigier, F., Rousseau, S., Coutanceau, C., Leger, J.-M., and Lamy, C. (2006) Electrocatalysis for the direct alcohol fuel cell. *Topics in Catalysis*, **40** (1), 111–121.

68 Liu, P., Logadottir, A., and Nørskov, J.K. (2003) Modeling the electro-oxidation of CO and H_2/CO on Pt, Ru, PtRu and Pt_3Sn. *Electrochimica Acta*, **48** (25–26), 3731–3742.

69 de Souza, J.P.I., Queiroz, S.L., Bergamaski, K., Gonzalez, E.R., and Nart, F.C. (2002) Electro-oxidation of ethanol on Pt, Rh, and PtRh electrodes: a study using DEMS and *in-situ* FTIR techniques. *The Journal of Physical Chemistry B*, **106** (38), 9825–9830.

70 Colmati, F., Antolini, E., and Gonzalez, E.R. (2008) Preparation, structural characterization and activity for ethanol oxidation of carbon supported ternary Pt–Sn–Rh catalysts. *Journal of Alloys and Compounds*, **456** (1–2), 264–270.

71 Kowal, A., Li, M., Shao, M., Sasaki, K., Vukmirovic, M.B., Zhang, J., Marinkovic, N.S., Liu, P., Frenkel, A.I., and Adzic, R.R. (2009) Ternary Pt/Rh/SnO_2 electrocatalysts for oxidizing ethanol to CO_2. *Nature Materials*, **8** (4), 325–330.

72 Spendelow, J.S. and Wieckowski, A. (2007) Electrocatalysis of oxygen reduction and small alcohol oxidation in alkaline media. *Physical Chemistry Chemical Physics*, **9** (21), 2654–2675.

73 Varcoe, J.R. and Slade, R.C.T. (2005) Prospects for alkaline anion-exchange membranes in low temperature fuel cells. *Fuel Cells*, **5** (2), 187–200.

74 Yanagi, H. and Fukuta, K. (2008) Anion exchange membrane and ionomer for alkaline membrane fuel cells (AMFCs). *ECS Transactions*, **16** (2), 257–262.

75 Blizanac, B.B., Ross, P.N., and Markovic, N.M. (2007) Oxygen electroreduction on Ag(1 1 1): the pH effect. *Electrochimica Acta*, **52** (6), 2264–2271.

76 Li, X., Popov, B.N., Kawahara, T., and Yanagi, H. (2011) Non-precious metal catalysts synthesized from precursors of carbon, nitrogen, and transition metal for

oxygen reduction in alkaline fuel cells. *Journal of Power Sources*, **196** (4), 1717–1722.

77 Xu, H. and Hou, X. (2007) Synergistic effect of modified Pt/C electrocatalysts on the performance of PEM fuel cells. *International Journal of Hydrogen Energy*, **32** (17), 4397–4401.

78 Cui, G., Song, S., Shen, P.K., Kowal, A., and Bianchini, C. (2009) First-principles considerations on catalytic activity of Pd toward ethanol oxidation. *The Journal of Physical Chemistry C*, **113** (35), 15639–15642.

79 Liang, Z.X., Zhao, T.S., Xu, J.B., and Zhu, L.D. (2009) Mechanism study of the ethanol oxidation reaction on palladium in alkaline media. *Electrochimica Acta*, **54** (8), 2203–2208.

80 Chen, Y., Zhuang, L., and Lu, J. (2007) Non-Pt anode catalysts for alkaline direct alcohol fuel cells. *Chinese Journal of Catalysis*, **28** (10), 870–874.

81 He, Q., Chen, W., Mukerjee, S., Chen, S., and Laufek, F. (2009) Carbon-supported PdM (M=Au and Sn) nanocatalysts for the electrooxidation of ethanol in high pH media. *Journal of Power Sources*, **187** (2), 298–304.

82 Shen, P.K. and Xu, C. (2006) Alcohol oxidation on nanocrystalline oxide Pd/C promoted electrocatalysts. *Electrochemistry Communications*, **8** (1), 184–188.

83 Bianchini, C., Bambagioni, V., Filippi, J., Marchionni, A., Vizza, F., Bert, P., and Tampucci, A. (2009) Selective oxidation of ethanol to acetic acid in highly efficient polymer electrolyte membrane-direct ethanol fuel cells. *Electrochemistry Communications*, **11** (5), 1077–1080.

84 Bambagioni, V., Bevilacqua, M., Filippi, J., Marchionni, A., Moneti, S., Vizza, F., and Bianchini, C. (2010) Direct alcohol fuel cells as chemical reactors for the sustainable production of energy and chemicals: energy and chemicals from renewables by electrocatalysis. *Chemistry Today*, **28** (3), 518–528.

85 Santasalo-Aarnio, A., Kwon, Y., Ahlberg, E., Kontturi, K., Kallio, T., and Koper, M.T.M. (2011) Comparison of methanol, ethanol and iso-propanol oxidation on Pt and Pd electrodes in alkaline media studied by HPLC. *Electrochemistry Communications*, **13** (5), 466–469.

86 Kwon, Y. and Koper, M.T.M. (2010) Combining voltammetry with HPLC: application to electro-oxidation of glycerol. *Analytical Chemistry*, **82** (13), 5420–5424.

87 Kwon, Y., Lai, S.C.S., Rodriguez, P., and Koper, M.T.M. (2011) Electrocatalytic oxidation of alcohols on gold in alkaline media: base or gold catalysis? *Journal of the American Chemical Society*, **133** (18), 6914–6917.

88 Roquet, L., Belgsir, E.M., Léger, J.M., and Lamy, C. (1994) Kinetics and mechanisms of the electrocatalytic oxidation of glycerol as investigated by chromatographic analysis of the reaction products: potential and pH effects. *Electrochimica Acta*, **39** (16), 2387–2394.

89 Zope, B.N., Hibbitts, D.D., Neurock, M., and Davis, R.J. (2010) Reactivity of the gold/water interface during selective oxidation catalysis. *Science*, **330** (6000), 74–78.

90 Demarconnay, L., Brimaud, S., Coutanceau, C., and Léger, J.M. (2007) Ethylene glycol electrooxidation in alkaline medium at multi-metallic Pt based catalysts. *Journal of Electroanalytical Chemistry*, **601** (1–2), 169–180.

91 Matsuoka, K., Iriyama, Y., Abe, T., Matsuoka, M., and Ogumi, Z. (2005) Electro-oxidation of methanol and ethylene glycol on platinum in alkaline solution: poisoning effects and product analysis. *Electrochimica Acta*, **51** (6), 1085–1090.

92 Chang, S.C., Ho, Y., and Weaver, M.J. (1991) Applications of real-time FTIR spectroscopy to the elucidation of complex electroorganic pathways: electrooxidation of ethylene glycol on gold, platinum, and nickel in alkaline solution. *Journal of the American Chemical Society*, **113** (25), 9506–9513.

93 Kohlmüller, H. (1976) Anodic oxidation of ethylene glycol with noble metal alloy catalysts. *Journal of Power Sources*, **1** (3), 249–256.

94 Kadirgan, F., Beden, B., and Lamy, C. (1983) Electrocatalytic oxidation of ethylene-glycol: Part II. Behaviour of platinum-ad-atom electrodes in alkaline medium. *Journal of Electroanalytical Chemistry and Interfacial Electrochemistry*, **143** (1–2), 135–152.

95 Dalbay, N. and Kadirgan, F. (1991) Electrolytically co-deposited platinum: palladium electrodes and their electrocatalytic activity for ethylene glycol oxidation – a synergistic effect. *Electrochimica Acta*, **36** (2), 353–356.

96 Simões, M., Baranton, S., and Coutanceau, C. (2010) Electro-oxidation of glycerol at Pd based nano-catalysts for an application in alkaline fuel cells for chemicals and energy cogeneration. *Applied Catalysis B: Environmental*, **93** (3–4), 354–362.

97 Bambagioni, V., Bevilacqua, M., Bianchini, C., Filippi, J., Lavacchi, A., Marchionni, A., Vizza, F., and Shen, P.K. (2010) Self-sustainable production of hydrogen, chemicals, and energy from renewable alcohols by electrocatalysis. *ChemSusChem*, **3** (7), 851–855.

98 Besson, M. and Gallezot, P. (2000) Selective oxidation of alcohols and aldehydes on metal catalysts. *Catalysis Today*, **57** (1–2), 127–141.

99 Mallat, T. and Baiker, A. (2004) Oxidation of alcohols with molecular oxygen on solid catalysts. *Chemical Reviews*, **104** (6), 3037–3058.

100 Ketchie, W.C., Fang, Y.-L., Wong, M.S., Murayama, M., and Davis, R.J. (2007) Influence of gold particle size on the aqueous-phase oxidation of carbon monoxide and glycerol. *Journal of Catalysis*, **250** (1), 94–101.

101 Corma, A. and Garcia, H. (2008) Supported gold nanoparticles as catalysts for organic reactions. *Chemical Society Reviews*, **37** (9), 2096–2126.

102 Della Pina, C., Falletta, E., Prati, L., and Rossi, M. (2008) Selective oxidation using gold. *Chemical Society Reviews*, **37** (9), 2077–2095.

103 Hutchings, G.J. (2008) Nanocrystalline gold and gold palladium alloy catalysts for chemical synthesis. *Chemical Communications*, (10), 1148–1164.

104 Zhou, C.-H., Beltramini, J.N., Fan, Y.-X., and Lu, G.Q. (2008) Chemoselective catalytic conversion of glycerol as a biorenewable source to valuable commodity chemicals. *Chemical Society Reviews*, **37** (3), 527–549.

105 Dimitratos, N., Lopez-Sanchez, J., and Hutchings, G. (2009) Green catalysis with alternative feedstocks. *Topics in Catalysis*, **52** (3), 258–268.

106 Carrettin, S., McMorn, P., Johnston, P., Griffin, K., and Hutchings, G.J. (2002) Selective oxidation of glycerol to glyceric acid using a gold catalyst in aqueous sodium hydroxide. *Chemical Communications*, (7), 696–697.

107 Carrettin, S., McMorn, P., Johnston, P., Griffin, K., Kiely, C.J., and Hutchings, G.J. (2003) Oxidation of glycerol using supported Pt, Pd and Au catalysts. *Physical Chemistry Chemical Physics*, **5** (6), 1329–1336.

108 Matsuoka, K., Iriyama, Y., Abe, T., Matsuoka, M., and Ogumi, Z. (2005) Alkaline direct alcohol fuel cells using an anion exchange membrane. *Journal of Power Sources*, **150** (0), 27–31.

109 Stamenkovic, V.R., Fowler, B., Mun, B.S., Wang, G., Ross, P.N., Lucas, C.A., and Marković, N.M. (2007) Improved oxygen reduction activity on $Pt_3Ni(111)$ via increased surface site availability. *Science*, **315** (5811), 493–497.

110 Marković, N.M. and Ross, P.N., Jr. (2002) Surface science studies of model fuel cell electrocatalysts. *Surface Science Reports*, **45** (4–6), 117–229.

111 Tian, N., Zhou, Z.-Y., and Sun, S.-G. (2008) Platinum metal catalysts of high-index surfaces: from single-crystal planes to electrochemically shape-controlled nanoparticles. *The Journal of Physical Chemistry C*, **112** (50), 19801–19817.

112 Arenz, M., Stamenkovic, V., Schmidt, T.J., Wandelt, K., Ross, P.N., and Markovic, N.M. (2003) The electro-oxidation of formic acid on Pt-Pd single crystal bimetallic surfaces. *Physical Chemistry Chemical Physics*, **5** (19), 4242–4251.

113 Somorjai, G.A. (1994) *Introduction to Surface Chemistry and Catalysis*, John Wiley & Sons, Inc., New York.

114 Lebedeva, N.P., Koper, M.T.M., Herrero, E., Feliu, J.M., and van Santen, R.A. (2000) Cooxidation on stepped Pt[*n*(111) × (111)] electrodes. *Journal of Electroanalytical Chemistry*, **487** (1), 37–44.

115 Stamenkovic, V.R., Mun, B.S., Arenz, M., Mayrhofer, K.J.J., Lucas, C.A., Wang, G., Ross, P.N., and Markovic, N.M. (2007) Trends in electrocatalysis on extended and nanoscale Pt-bimetallic alloy surfaces. *Nature Materials*, **6** (3), 241–247.

116 Ralph, T.R. and Hogarth, M.P. (2002) Catalysis for low temperature fuel cells Part 1: the cathode challenges. *Platinum Metals Review*, **46** (1), 3–14.

117 Ermete, A. (2003) Formation of carbon-supported PtM alloys for low temperature fuel cells: a review. *Materials Chemistry and Physics*, **78** (3), 563–573.

118 Somorjai, G., Tao, F., and Park, J. (2008) The nanoscience revolution: merging of colloid science, catalysis and nanoelectronics. *Topics in Catalysis*, **47** (1), 1–14.

119 Borup, R., Meyers, J., Pivovar, B., Kim, Y.S., Mukundan, R., Garland, N., Myers, D., Wilson, M., Garzon, F., Wood, D., Zelenay, P., More, K., Stroh, K., Zawodzinski, T., Boncella, J., McGrath, J.E., Inaba, M., Miyatake, K., Hori, M., Ota, K., Ogumi, Z., Miyata, S., Nishikata, A., Siroma, Z., Uchimoto, Y., Yasuda, K., Kimijima, K.-I., and Iwashita, N. (2007) Scientific aspects of polymer electrolyte fuel cell durability and degradation. *Chemical Reviews*, **107** (10), 3904–3951.

120 Chan, K.-Y., Ding, J., Ren, J., Cheng, S., and Tsang, K.Y. (2004) Supported mixed metal nanoparticles as electrocatalysts in low temperature fuel cells. *Journal of Materials Chemistry*, **14** (4), 505–516.

121 Sasaki, T., Koshizaki, N., Terauchi, S., Umehara, H., Matsumoto, Y., and Koinuma, M. (1997) Preparation of Pt/TiO_2 nanocomposite films using co-sputtering method. *Nanostructured Materials*, **8** (8), 1077–1083.

122 Yan, X.M., Ni, J., Robbins, M., Park, H.J., Zhao, W., and White, J.M. (2002) Silver nanoparticles synthesized by vapor deposition onto an ice matrix. *Journal of Nanoparticle Research*, **4** (6), 525–533.

123 Debe, M.K., Schmoeckel, A.K., Vernstrom, G.D., and Atanasoski, R. (2006) High voltage stability of nanostructured thin film catalysts for PEM fuel cells. *Journal of Power Sources*, **161** (2), 1002–1011.

124 Astruc, D. (2008) *Nanoparticles and Catalysis*, Wiley-VCH Verlag GmbH, Weinheim.

125 Ahmadi, T.S., Wang, Z.L., Green, T.C., Henglein, A., and El-Sayed, M.A. (1996) Shape-controlled synthesis of colloidal platinum nanoparticles. *Science*, **272** (5270), 1924–1925.

126 Toshima, N. and Yonezawa, T. (1998) Bimetallic nanoparticles-novel materials for chemical and physical applications. *New Journal of Chemistry*, **22** (11), 1179–1201.

127 Crooks, R.M., Zhao, M., Sun, L., Chechik, V., and Yeung, L.K. (2000) Dendrimer-encapsulated metal nanoparticles: synthesis, characterization, and applications to catalysis. *Accounts of Chemical Research*, **34** (3), 181–190.

128 Murray, C.B., Kagan, C.R., and Bawendi, M.G. (2000) Synthesis and characterization of monodisperse nanocrystals and close-packed nanocrystal assemblies. *Annual Review of Materials Science*, **30**, 545–610.

129 Sun, S., Murray, C.B., Weller, D., Folks, L., and Moser, A. (2000) Monodisperse FePt nanoparticles and ferromagnetic FePt nanocrystal superlattices. *Science*, **287** (5460), 1989–1992.

130 Bönnemann, H. and Richards, R.M. (2001) Nanoscopic metal particles: synthetic methods and potential applications. *European Journal of Inorganic Chemistry*, **2001** (10), 2455–2480.

131 Jana, N.R., Gearheart, L., and Murphy, C.J. (2001) Seed-mediated growth approach for shape-controlled synthesis of spheroidal and rod-like gold nanoparticles using a surfactant template. *Advanced Materials*, **13** (18), 1389–1393.

132 Roucoux, A., Schulz, J., and Patin, H. (2002) Reduced transition metal colloids:

a novel family of reusable catalysts? *Chemical Reviews*, **102** (10), 3757–3778.

133 Sun, Y. and Xia, Y. (2002) Shape-controlled synthesis of gold and silver nanoparticles. *Science*, **298** (5601), 2176–2179.

134 Wang, C., Hou, Y., Kim, J., and Sun, S. (2007) A general strategy for synthesizing FePt nanowires and nanorods. *Angewandte Chemie: International Edition*, **46** (33), 6333–6335.

135 Alayoglu, S., Nilekar, A.U., Mavrikakis, M., and Eichhorn, B. (2008) Ru-Pt core–shell nanoparticles for preferential oxidation of carbon monoxide in hydrogen. *Nature Materials*, **7** (4), 333–338.

136 Somorjai, G. and Park, J. (2008) Colloid science of metal nanoparticle catalysts in 2D and 3D structures: challenges of nucleation, growth, composition, particle shape, size control and their influence on activity and selectivity. *Topics in Catalysis*, **49** (3), 126–135.

137 Wang, C., Daimon, H., Onodera, T., Koda, T., and Sun, S. (2008) A general approach to the size- and shape-controlled synthesis of platinum nanoparticles and their catalytic reduction of oxygen. *Angewandte Chemie*, **120** (19), 3644–3647.

138 Chen, J., Lim, B., Lee, E.P., and Xia, Y. (2009) Shape-controlled synthesis of platinum nanocrystals for catalytic and electrocatalytic applications. *Nano Today*, **4** (1), 81–95.

139 Lim, B., Jiang, M., Camargo, P.H.C., Cho, E.C., Tao, J., Lu, X., Zhu, Y., and Xia, Y. (2009) Pd-Pt bimetallic nanodendrites with high activity for oxygen reduction. *Science*, **324** (5932), 1302–1305.

140 Xie, X., Li, Y., Liu, Z.-Q., Haruta, M., and Shen, W. (2009) Low-temperature oxidation of CO catalysed by Co_3O_4 nanorods. *Nature*, **458** (7239), 746–749.

141 Zhang, J., Vukmirovic, M.B., Xu, Y., Mavrikakis, M., and Adzic, R.R. (2005) Controlling the catalytic activity of platinum-monolayer electrocatalysts for oxygen reduction with different substrates. *Angewandte Chemie: International Edition*, **44** (14), 2132–2135.

142 Zhang, J., Sasaki, K., Sutter, E., and Adzic, R.R. (2007) Stabilization of platinum oxygen-reduction electrocatalysts using gold clusters. *Science*, **315** (5809), 220–222.

143 Goodenough, J.B., Hamnett, A., Kennedy, B.J., Manoharan, R., and Weeks, S.A. (1990) Porous carbon anodes for the direct methanol fuel cell: I. The role of the reduction method for carbon supported platinum electrodes. *Electrochimica Acta*, **35** (1), 199–207.

144 Román-Martínez, M.C., Cazorla-Amorós, D., Yamashita, H., and de Miguel, S., and Scelza, O.A. (1999) XAFS study of dried and reduced PtSn/C catalysts: nature and structure of the catalytically active phase. *Langmuir*, **16** (3), 1123–1131.

145 Takasu, Y., Fujiwara, T., Murakami, Y., Sasaki, K., Oguri, M., Asaki, T., and Sugimoto, W. (2000) Effect of structure of carbon-supported PtRu electrocatalysts on the electrochemical oxidation of methanol. *Journal of the Electrochemical Society*, **147** (12), 4421–4427.

146 Boxall, D.L., Deluga, G.A., Kenik, E.A., King, W.D., and Lukehart, C.M. (2001) Rapid synthesis of a Pt_1Ru_1/carbon nanocomposite using microwave irradiation: a DMFC anode catalyst of high relative performance. *Chemistry of Materials*, **13** (3), 891–900.

147 Joo, S.H., Choi, S.J., Oh, I., Kwak, J., Liu, Z., Terasaki, O., and Ryoo, R. (2001) Ordered nanoporous arrays of carbon supporting high dispersions of platinum nanoparticles. *Nature*, **412** (6843), 169–172.

148 Dickinson, A.J., Carrette, L.P.L., Collins, J.A., Friedrich, K.A., and Stimming, U. (2002) Preparation of a Pt-Ru/C catalyst from carbonyl complexes for fuel cell applications. *Electrochimica Acta*, **47** (22–23), 3733–3739.

149 Fujiwara, N., Yasuda, K., Ioroi, T., Siroma, Z., and Miyazaki, Y. (2002) Preparation of platinum–ruthenium onto solid polymer electrolyte membrane and the application to a DMFC anode. *Electrochimica Acta*, **47** (25), 4079–4084.

150 Pozio, A., Silva, R.F., De Francesco, M., Cardellini, F., and Giorgi, L. (2002) A

novel route to prepare stable Pt-Ru/C electrocatalysts for polymer electrolyte fuel cell. *Electrochimica Acta*, **48** (3), 255–262.

151 Steigerwalt, E.S., Deluga, G.A., and Lukehart, C.M. (2002) Pt-Ru/carbon fiber nanocomposites: synthesis, characterization, and performance as anode catalysts of direct methanol fuel cells. A search for exceptional performance. *The Journal of Physical Chemistry B*, **106** (4), 760–766.

152 Xiong, L., Kannan, A.M., and Manthiram, A. (2002) Pt–M (M=Fe, Co, Ni and Cu) electrocatalysts synthesized by an aqueous route for proton exchange membrane fuel cells. *Electrochemistry Communications*, **4** (11), 898–903.

153 Venkataraman, R., Kunz, H.R., and Fenton, J.M. (2003) Development of new CO tolerant ternary anode catalysts for proton exchange membrane fuel cells. *Journal of the Electrochemical Society*, **150** (3), A278–A284.

154 Kawaguchi, T., Sugimoto, W., Murakami, Y., and Takasu, Y. (2004) Temperature dependence of the oxidation of carbon monoxide on carbon supported Pt, Ru, and PtRu. *Electrochemistry Communications*, **6** (5), 480–483.

155 Lizcano-Valbuena, W.H., de Azevedo, D.C., and Gonzalez, E.R. (2004) Supported metal nanoparticles as electrocatalysts for low-temperature fuel cells. *Electrochimica Acta*, **49** (8), 1289–1295.

156 Vigier, F., Coutanceau, C., Perrard, A., Belgsir, E.M., and Lamy, C. (2004) Development of anode catalysts for a direct ethanol fuel cell. *Journal of Applied Electrochemistry*, **34** (4), 439–446.

157 Li, W., Sun, G., Yan, Y., and Xin, Q. (2005) Supported noble metal electrocatalysts in low temperature fuel cells. *Progress in Chemistry*, **17** (5), 761–772.

158 Cui, Z., Liu, C., Liao, J., and Xing, W. (2008) Highly active PtRu catalysts supported on carbon nanotubes prepared by modified impregnation method for methanol electro-oxidation. *Electrochimica Acta*, **53** (27), 7807–7811.

159 Watanabe, M., Uchida, M., and Motoo, S. (1987) Preparation of highly dispersed Pt + Ru alloy clusters and the activity for the electrooxidation of methanol. *Journal of Electroanalytical Chemistry and Interfacial Electrochemistry*, **229** (1–2), 395–406.

160 Götz, M. and Wendt, H. (1998) Binary and ternary anode catalyst formulations including the elements W, Sn and Mo for PEMFCs operated on methanol or reformate gas. *Electrochimica Acta*, **43** (24), 3637–3644.

161 Hirai, H., Nakao, Y., and Toshima, N. (1979) Preparation of colloidal transition metals in polymers by reduction with alcohols or ethers. *Journal of Macromolecular Science: Part A – Chemistry*, **13** (6), 727–750.

162 Toshima, N., Yonezawa, T., and Kushihashi, K. (1993) Polymer-protected palladium–platinum bimetallic clusters: preparation, catalytic properties and structural considerations. *Journal of the Chemical Society, Faraday Transactions*, **89** (14), 2537–2543.

163 Camargo, P.H.C., Xiong, Y., Ji, L., Zuo, J.M., and Xia, Y. (2007) Facile synthesis of tadpole-like nanostructures consisting of Au heads and Pd tails. *Journal of the American Chemical Society*, **129** (50), 15452–15453.

164 Xiong, Y., Cai, H., Wiley, B.J., Wang, J., Kim, M.J., and Xia, Y. (2007) Synthesis and mechanistic study of palladium nanobars and nanorods. *Journal of the American Chemical Society*, **129** (12), 3665–3675.

165 Wang, Y., Ren, J., Deng, K., Gui, L., and Tang, Y. (2000) Preparation of tractable platinum, rhodium, and ruthenium nanoclusters with small particle size in organic media. *Chemistry of Materials*, **12** (6), 1622–1627.

166 Li, W., Liang, C., Qiu, J., Zhou, W., Han, H., Wei, Z., Sun, G., and Xin, Q. (2002) Carbon nanotubes as support for cathode catalyst of a direct methanol fuel cell. *Carbon*, **40** (5), 791–794.

167 Liu, Z., Lee, J.Y., Chen, W., Han, M., and Gan, L.M. (2003) Physical and electrochemical characterizations of microwave-assisted polyol preparation of

carbon-supported PtRu nanoparticles. *Langmuir*, **20** (1), 181–187.

168 Zhou, Z., Wang, S., Zhou, W., Wang, G., Jiang, L., Li, W., Song, S., Liu, J., Sun, G., and Xin, Q. (2003) Novel synthesis of highly active Pt/C cathode electrocatalyst for direct methanol fuel cell. *Chemical Communications*, (3), 394–395.

169 Bock, C., Paquet, C., Couillard, M., Botton, G.A., and MacDougall, B.R. (2004) Size-selected synthesis of PtRu nano-catalysts: reaction and size control mechanism. *Journal of the American Chemical Society*, **126** (25), 8028–8037.

170 Jiang, L., Zhou, Z., Li, W., Zhou, W., Song, S., Li, H., Sun, G., and Xin, Q. (2004) Effects of treatment in different atmosphere on Pt_3Sn/C electrocatalysts for ethanol electro-oxidation. *Energy & Fuels*, **18** (3), 866–871.

171 Li, H., Xin, Q., Li, W., Zhou, Z., Jiang, L., Yang, S., and Sun, G. (2004) An improved palladium-based DMFCs cathode catalyst. *Chemical Communications*, (23), 2776–2777.

172 Li, W., Liang, C., Qiu, J., Li, H., Zhou, W., Sun, G., and Xin, Q. (2004) Multi-walled carbon nanotubes supported Pt-Fe cathodic catalyst for direct methanol fuel cell. *Reaction Kinetics and Catalysis Letters*, **82** (2), 235–240.

173 Li, W., Zhou, W., Li, H., Zhou, Z., Zhou, B., Sun, G., and Xin, Q. (2004) Nano-structured Pt–Fe/C as cathode catalyst in direct methanol fuel cell. *Electrochimica Acta*, **49** (7), 1045–1055.

174 Xing, Y. (2004) Synthesis and electrochemical characterization of uniformly-dispersed high loading Pt nanoparticles on sonochemically-treated carbon nanotubes. *The Journal of Physical Chemistry B*, **108** (50), 19255–19259.

175 Li, W., Wang, X., Chen, Z., Waje, M., and Yan, Y. (2005) Carbon nanotube film by filtration as cathode catalyst support for proton-exchange membrane fuel cell. *Langmuir*, **21** (21), 9386–9389.

176 Chen, Z., Xu, L., Li, W., Waje, M., and Yan, Y. (2006) Polyaniline nanofibre supported platinum nanoelectrocatalysts for direct methanol fuel cells. *Nanotechnology*, **17** (20), 5254.

177 Li, W., Wang, X., Chen, Z., Waje, M., and Yan, Y. (2006) Pt-Ru supported on double-walled carbon nanotubes as high-performance anode catalysts for direct methanol fuel cells. *The Journal of Physical Chemistry B*, **110** (31), 15353–15358.

178 Knupp, S.L., Li, W., Paschos, O., Murray, T.M., Snyder, J., and Haldar, P. (2008) The effect of experimental parameters on the synthesis of carbon nanotube/nanofiber supported platinum by polyol processing techniques. *Carbon*, **46** (10), 1276–1284.

179 Avasarala, B., Murray, T., Li, W., and Haldar, P. (2009) Titanium nitride nanoparticles based electrocatalysts for proton exchange membrane fuel cells. *Journal of Materials Chemistry*, **19** (13), 1803–1805.

180 Sun, S. and Zeng, H. (2002) Size-controlled synthesis of magnetite nanoparticles. *Journal of the American Chemical Society*, **124** (28), 8204–8205.

181 Liu, Z., Ada, E.T., Shamsuzzoha, M., Thompson, G.B., and Nikles, D.E. (2006) Synthesis and activation of PtRu alloyed nanoparticles with controlled size and composition. *Chemistry of Materials*, **18** (20), 4946–4951.

182 Luo, J., Njoki, P.N., Lin, Y., Mott, D., and Wang, L.Y., and Zhong, C.-J. (2006) Characterization of carbon-supported AuPt nanoparticles for electrocatalytic methanol oxidation reaction. *Langmuir*, **22** (6), 2892–2898.

183 Yano, H., Kataoka, M., Yamashita, H., Uchida, H., and Watanabe, M. (2007) Oxygen reduction activity of carbon-supported Pt-M (M=V, Ni, Cr, Co, and Fe) alloys prepared by nanocapsule method. *Langmuir*, **23** (11), 6438–6445.

184 Li, W. and Haldar, P. (2009) Supportless PdFe nanorods as highly active electrocatalyst for proton exchange membrane fuel cell. *Electrochemistry Communications*, **11** (6), 1195–1198.

185 Li, W., Chen, Z., Xu, L., and Yan, Y. (2010) A solution-phase synthesis method to highly active Pt-Co/C electrocatalysts for proton exchange membrane fuel cell. *Journal of Power Sources*, **195** (9), 2534–2540.

186 Zhang, Z., More, K.L., Sun, K., Wu, Z., and Li, W. (2011) Preparation and characterization of PdFe nanoleaves as electrocatalysts for oxygen reduction reaction. *Chemistry of Materials*, **23** (6), 1570–1577.

187 Zhang, Z., Xin, L., Sun, K., and Li, W. (2011) Pd–Ni electrocatalysts for efficient ethanol oxidation reaction in alkaline electrolyte. *International Journal of Hydrogen Energy*, **36** (20), 12686–12697.

188 Zhang, Z., Li, M., Wu, Z., and Li, W. (2011) Ultra-thin PtFe-nanowires as durable electrocatalysts for fuel cells. *Nanotechnology*, **22** (1), 015602.

189 Shinoda, K. and Friberg, S. (1975) Microemulsions: colloidal aspects. *Advances in Colloid and Interface Science*, **4** (4), 281–300.

190 Bommarius, A.S., Holzwarth, J.F., Wang, D.I.C., and Hatton, T.A. (1990) Coalescence and solubilizate exchange in a cationic four-component reversed micellar system. *The Journal of Physical Chemistry*, **94** (18), 7232–7239.

191 Wang, J., Ee, L.S., Ng, S.C., Chew, C.H., and Gan, L.M. (1997) Reduced crystallization temperature in a microemulsion-derived zirconia precursor. *Materials Letters*, **30** (1), 119–124.

192 Wu, M.-L., Chen, D.-H., and Huang, T.-C. (2001) Preparation of Au/Pt bimetallic nanoparticles in water-in-oil microemulsions. *Chemistry of Materials*, **13** (2), 599–606.

193 Liu, Z., Lee, J.Y., Han, M., Chen, W., and Gan, L.M. (2002) Synthesis and characterization of PtRu/C catalysts from microemulsions and emulsions. *Journal of Materials Chemistry*, **12** (8), 2453–2458.

194 Zhang, X. and Chan, K.-Y. (2002) Water-in-oil microemulsion synthesis of platinum–ruthenium nanoparticles, their characterization and electrocatalytic properties. *Chemistry of Materials*, **15** (2), 451–459.

195 Rojas, S., García-García, F.J., Järas, S., Martínez-Huerta, M.V., Fierro, J.L.G., and Boutonnet, M. (2005) Preparation of carbon supported Pt and PtRu nanoparticles from microemulsion: electrocatalysts for fuel cell applications. *Applied Catalysis A: General*, **285** (1–2), 24–35.

196 Xiong, L. and Manthiram, A. (2005) Catalytic activity of Pt–Ru alloys synthesized by a microemulsion method in direct methanol fuel cells. *Solid State Ionics*, **176** (3–4), 385–392.

197 Lei, H., Atanassova, P., Sun, Y., and Blizanac, B. (2009) State-of-the-art electrocatalysts for direct methanol fuel cells, in *Electrocatalysis of Direct Methanol Fuel Cells:From Fundamentals to Applications* (eds. H. Liu and J. Zhang), Wiley-VCH Verlag GmbH, Weinheim, pp. 197–226.

198 Shao-Horn, Y., Ferreira, P., and la O, G.J. (2006) Instability of Pt/C electrocatalysts in proton exchange membrane fuel cells: a mechanistic investigation. *ECS Meeting Abstracts*, **503** (2), 200.

199 Iijima, S. (1991) Helical microtubules of graphitic carbon. *Nature*, **354** (6348), 56–58.

200 Che, G., Lakshmi, B.B., Fisher, E.R., and Martin, C.R. (1998) Carbon nanotubule membranes for electrochemical energy storage and production. *Nature*, **393** (6683), 346–349.

201 Britto, P.J., Santhanam, K.S.V., Rubio, A., Alonso, J.A., and Ajayan, P.M. (1999) Improved charge transfer at carbon nanotube electrodes. *Advanced Materials*, **11** (2), 154–157.

202 Li, W., Liang, C., Zhou, W., Qiu, J., Zhenhua, Sun, G., and Xin, Q. (2003) Preparation and characterization of multiwalled carbon nanotube-supported platinum for cathode catalysts of direct methanol fuel cells. *The Journal of Physical Chemistry B*, **107** (26), 6292–6299.

203 Rajesh, B., Ravindranathan Thampi, K., Bonard, J.M., Xanthopoulos, N., Mathieu, H.J., and Viswanathan, B. (2003) Carbon nanotubes generated from template carbonization of polyphenyl acetylene as the support for electrooxidation of methanol. *The Journal of Physical Chemistry B*, **107** (12), 2701–2708.

204 Sun, X., Li, R., Villers, D., Dodelet, J.P., and Désilets, S. (2003) Composite electrodes made of Pt nanoparticles

deposited on carbon nanotubes grown on fuel cell backings. *Chemical Physics Letters*, **379** (1–2), 99–104.

205 Wang, C., Waje, M., Wang, X., Tang, J.M., Haddon, R.C., and Yushan (2003) Proton exchange membrane fuel cells with carbon nanotube based electrodes. *Nano Letters*, **4** (2), 345–348.

206 Li, L. and Xing, Y. (2007) Pt–Ru nanoparticles supported on carbon nanotubes as methanol fuel cell catalysts. *The Journal of Physical Chemistry C*, **111** (6), 2803–2808.

207 Wang, X., Li, W., Chen, Z., Waje, M., and Yan, Y. (2006) Durability investigation of carbon nanotube as catalyst support for proton exchange membrane fuel cell. *Journal of Power Sources*, **158** (1), 154–159.

208 Bessel, C.A., Laubernds, K., Rodriguez, N.M., and Baker, R.T.K. (2001) Graphite nanofibers as an electrode for fuel cell applications. *Journal of Physical Chemistry B*, **105** (6), 1115–1118.

209 Serp, P., Corrias, M., and Kalck, P. (2003) Carbon nanotubes and nanofibers in catalysis. *Applied Catalysis A: General*, **253** (2), 337–358.

210 Guo, J., Sun, G., Wang, Q., Wang, G., Zhou, Z., Tang, S., Jiang, L., Zhou, B., and Xin, Q. (2006) Carbon nanofibers supported Pt–Ru electrocatalysts for direct methanol fuel cells. *Carbon*, **44** (1), 152–157.

211 Lee, K., Zhang, J., Wang, H., and Wilkinson, D.P. (2006) Progress in the synthesis of carbon nanotube- and nanofiber-supported Pt electrocatalysts for PEM fuel cell catalysis. *Journal of Applied Electrochemistry*, **36** (5), 507–522.

212 Hsin, Y.L., Hwang, K.C., and Yeh, C.-T. (2007) Poly(vinylpyrrolidone)-modified graphite carbon nanofibers as promising supports for PtRu catalysts in direct methanol fuel cells. *Journal of the American Chemical Society*, **129** (32), 9999–10010.

213 Chai, G.S., Yoon, S.B., Yu, J.-S., Choi, J.-H., and Sung, Y.-E. (2004) Ordered porous carbons with tunable pore sizes as catalyst supports in direct methanol fuel cell. *The Journal of Physical Chemistry B*, **108** (22), 7074–7079.

214 Lee, J., Yoon, S., Hyeon, T., Oh, S.M., and Bum Kim, K. (1999) Synthesis of a new mesoporous carbon and its application to electrochemical double-layer capacitors. *Chemical Communications*, (21), 2177–2178.

215 Ryoo, R., Joo, S.H., and Jun, S. (1999) Synthesis of highly ordered carbon molecular sieves via template-mediated structural transformation. *The Journal of Physical Chemistry B*, **103** (37), 7743–7746.

216 Lu, A.H. and Schüth, F. (2006) Nanocasting: a versatile strategy for creating nanostructured porous materials. *Advanced Materials*, **18** (14), 1793–1805.

217 Liang, C., Hong, K., Guiochon, G.A., Mays, J.W., and Dai, S. (2004) Synthesis of a large-scale highly ordered porous carbon film by self-assembly of block copolymers. *Angewandte Chemie: International Edition*, **43** (43), 5785–5789.

218 Meng, Y., Gu, D., Zhang, F., Shi, Y., Yang, H., Li, Z., Yu, C., Tu, B., and Zhao, D. (2005) Ordered mesoporous polymers and homologous carbon frameworks: amphiphilic surfactant templating and direct transformation. *Angewandte Chemie*, **117** (43), 7215–7221.

219 Tanaka, S., Nishiyama, N., Egashira, Y., and Ueyama, K. (2005) Synthesis of ordered mesoporous carbons with channel structure from an organic–organic nanocomposite. *Chemical Communications*, (16), 2125–2127.

220 Kim, H.-T., You, D.J., Yoon, H.-K., Joo, S.H., Pak, C., Chang, H., and Song, I.-S. (2008) Cathode catalyst layer using supported Pt catalyst on ordered mesoporous carbon for direct methanol fuel cell. *Journal of Power Sources*, **180** (2), 724–732.

221 Novoselov, K.S., Geim, A.K., Morozov, S.V., Jiang, D., Zhang, Y., Dubonos, S.V., Grigorieva, I.V., and Firsov, A.A. (2004) Electric field effect in atomically thin carbon films. *Science*, **306** (5696), 666–669.

222 Geim, A.K. and Novoselov, K.S. (2007) The rise of graphene. *Nature Materials*, **6** (3), 183–191.

223 Guo, S., Dong, S., and Wang, E. (2009) Three-dimensional Pt-on-Pd bimetallic nanodendrites supported on graphene nanosheet: facile synthesis and used as an advanced nanoelectrocatalyst for methanol oxidation. *ACS Nano*, **4** (1), 547–555.

224 Kou, R., Shao, Y., Wang, D., Engelhard, M. H., Kwak, J.H., Wang, J., Viswanathan, V. V., Wang, C., Lin, Y., Wang, Y., Aksay, I. A., and Liu, J. (2009) Enhanced activity and stability of Pt catalysts on functionalized graphene sheets for electrocatalytic oxygen reduction. *Electrochemistry Communications*, **11** (5), 954–957.

225 Li, Y., Tang, L., and Li, J. (2009) Preparation and electrochemical performance for methanol oxidation of Pt/graphene nanocomposites. *Electrochemistry Communications*, **11** (4), 846–849.

226 Seger, B. and Kamat, P.V. (2009) Electrocatalytically active graphene–platinum nanocomposites: role of 2-D carbon support in PEM fuel cells. *The Journal of Physical Chemistry C*, **113** (19), 7990–7995.

227 Yoo, E., Okata, T., Akita, T., Kohyama, M., Nakamura, J., and Honma, I. (2009) Enhanced electrocatalytic activity of Pt subnanoclusters on graphene nanosheet surface. *Nano Letters*, **9** (6), 2255–2259.

228 Zhang, Z.Y., Xin, L., and Li, W. (2012) Electrocatalytic oxidation of glycerol on Pt/C in anion-exchange membrane fuel cell: cogeneration of electricity and valuable chemicals. *Applied Catalysis B: Environmental*, **119**, 40–48.

229 Xin, L., Zhang, Z.Y., Qi, J., Chadderdon, D., and Li, W.Z. (2012) Electrocatalytic oxidation of ethylene glycol (EG) on supported Pt and Au catalysts in alkaline media: reaction pathway investigation in three-electrode cell and fuel cell reactors. *Applied Catalysis B: Environmental*, **125**, 85–94.

230 Zhang, Z.Y., Xin, L., and Li, W. (2012) Supported gold nanoparticles as anode catalyst for anion-exchange membrane-direct glycerol fuel cell (AEM-DGFC). *International Journal of Hydrogen Energy*, **37** (11), 9393–9401.

231 Xin, L., Zhang, Z.Y., Wang, Z.C., and Li, W.Z. (2012) Simultaneous generation of mesoxalic acid and electricity from glycerol on a gold anode catalyst in anion-exchange membrane fuel cells. *ChemCatChem*, **4** (8), 1105–1114.

232 Zhang, Z.Y., Xin, L., Qi, J., Chadderdon, D.J., Sun, K., Warsko, K.M., and Li, W.Z. (2014) Selective electro-oxidation of glycerol to tartronate or mesoxalate on Au nanoparticle catalyst via electrode potential tuning in anion-exchange membrane electro-catalytic flow reactor. *Applied Catalysis B: Environmental*, **147**, 871–878.

233 Qi, J., Xin, L., Chadderdon, D.J., Qiu, Y., Jiang, Y., Benipal, N., Liang, C.H., and Li, W.Z. (2014) Electrocatalytic selective oxidation of glycerol to tartronate on Au/C anode catalysts in anion exchange membrane fuel cells with electricity cogeneration. *Applied Catalysis B: Environmental*, **154**, 360–368.